eLife

Reviewed Preprint
v2 • November 28, 2024
Revised by authors

Reviewed Preprint
v1 • June 5, 2024

Developmental Biology

The autophagy protein, ATG14 safeguards against unscheduled pyroptosis activation to enable embryo transport during early pregnancy

Pooja Popli, Arin K Oestreich, Vineet K Maurya, Marina N Rowen, Yong Zhang, Michael J Holtzman, Ramya Masand, John Lydon, Shizuo Akira, Kelle H Moley, Ramakrishna Kommagani

Department of Pathology and Immunology, Baylor College of Medicine, Houston, USA • Department Obstetrics and Gynecology, Washington University School of Medicine, St. Louis, USA • Center for Reproductive Health Sciences, Washington University School of Medicine, St. Louis, USA • Department of Molecular and Cellular Biology, Baylor College of Medicine, Houston, USA • Department of Medicine and Department of Cell Biology, Washington University School of Medicine, St. Louis, USA • Department of Host Defense, Research Institute for Microbial Diseases (RIMD), Osaka University, Osaka, Japan • Laboratory of Host Defense, World Premier Institute Immunology Frontier Research Center (WPI-IFReC), Osaka University, Osaka, Japan • Department of Molecular Virology and Microbiology, Baylor College of Medicine, Houston, USA

eLife Assessment

This **valuable** study reports a novel function of ATG14 in preventing pyroptosis and inflammation in oviduct cells, thus allowing smooth transport of the early embryo to the uterus and implantation. The data supporting the main conclusion are **solid**. This work will be of interest to reproductive biologists and physicians practicing reproductive medicine.

https://doi.org/10.7554/eLife.97325.2.sa4

Abstract

Recurrent pregnancy loss (RPL), characterized by two or more failed clinical pregnancies, poses a significant challenge to reproductive health. In addition to embryo quality and endometrial function, proper oviduct function is also essential for successful pregnancy establishment. Therefore, structural abnormalities or inflammation resulting from infection in the oviduct may impede the transport of embryos to the endometrium, thereby increasing the risk of miscarriage. However, our understanding of the biological processes that preserve the oviductal cellular structure and functional integrity is limited. Here, we report that Atg14-dependent autophagy plays a crucial role in maintaining the cellular integrity of the oviduct by controlling inflammatory responses, thereby supporting efficient embryo transport. Specifically, the conditional depletion of the autophagy-related gene, *Atg14* in the oviduct causes severe structural abnormalities compromising its cellular integrity leading to the

abnormal retention of embryos. Interestingly, the selective loss of *Atg14* in oviduct ciliary epithelial cells did not impact female fertility, highlighting the specificity of ATG14 function in distinct cell types within the oviduct. Mechanistically, loss of *Atg14* triggered unscheduled pyroptosis via altering the mitochondrial integrity leading to inappropriate embryo retention and impeded embryo transport in the oviduct. Finally, pharmacological activation of pyroptosis in pregnant mice phenocopied the genetically induced defect and caused impairment in embryo transport. Together, we found that ATG14 safeguards against unscheduled pyroptosis activation to enable embryo transport from the oviduct to uterus for the successful implantation. Of clinical significance, these findings provide possible insights into the underlying mechanism(s) of early pregnancy loss and might aid in developing novel prevention strategies using autophagy modulators.

Introduction

A successful pregnancy is orchestrated by the sequential and coordinated events happening in the FRT [1]. Each of these events is crucial to advance to the next step in pregnancy. For example, as a first step, the ovary undergoes ovulation to release a mature ovum which is collected by oviduct fimbriae and funnelled through the infundibulum into the ampulla where they get fertilized by sperm. The embryos then pass through the ampulla-isthmus junction (AIJ) to enter the isthmus of the oviduct before exiting via the distal utero-tubal junction (UTJ) to implant on the wall of the uterus. Recently, the intricate structural and cellular diversity of the oviduct has drawn significant attention, emphasizing its vital role in facilitating embryo development and transport [2–4]. Morphologically, the oviduct is divided into four evolutionarily conserved regions: the infundibulum (nearest the ovary), ampulla (the site of fertilization), isthmus (serving as a sperm reservoir and site for early embryonic development), and utero-tubal junction (connected to the uterus). Each of these segments comprises epithelial, stromal, and smooth muscle cells with lumen lined up with an epithelium containing secretory ($PAX8^+$) and multi-ciliated ($FOXJ1^+$) cells. While the infundibulum and ampulla are composed of more ciliated than secretory cells, the isthmus has more secretory than ciliated cells [5, 6]. Successful pregnancy requires that the embryo transit the entire oviduct orchestrated by the following: (1) secretory cells producing oviduct fluid, (2) beating cilia to ensure unidirectional flow of the fluid, and (3) periodic contractions of surrounding muscle to propel fluid flow. Therefore, a combination of ciliary and muscular activity contributes to the overall success of oviduct embryo transport. This combination of ciliary and muscular activity plays a crucial role in the effective transport of the embryo through the oviduct. Any perturbations in these early pregnancy events can lead to adverse ripple effects that can compromise pregnancy outcomes. Previous studies have reported that impaired oviductal transport of embryos can lead to pregnancy failure and cause infertility in mice [7–10]. However, the underlying mechanism is not yet completely understood.

Autophagy is a cellular process, evolutionarily conserved from yeast to mammals, that recycles long-lived proteins and organelles to maintain cell energy homeostasis. Autophagy is classically activated through the nutrient sensor or mammalian target of the rapamycin complex. Genetic screens for autophagy-defective mutants in yeast and other fungi have currently identified 41 autophagy-related (ATG) genes that play a primary role in autophagy [11, 12]. Approximately half of these genes have homologs in higher organisms, and *Atg14* (also known as Barkor for Beclin 1 (*Becn1*)-associated autophagy-related key regulator) is one of them [13, 14]. ATG14 is part of a protein complex that is composed of Beclin 1, vacuolar sorting protein 15 (VPS15), and VPS34 (also named as Pik3c3, the catalytic subunit of the class III phosphatidylinositol 3-kinase), and this ATG14-containing complex plays an important role in the initiation process of autophagy.

Pyroptosis is a type of inflammatory cell death mediated by gasdermin (GSDM) and is a product of continuous cell expansion until the cytomembrane ruptures, resulting in the release of cellular contents that can activate strong inflammatory and immune responses. Gasdermin family proteins

are the primary executioners of pyroptosis. Cytotoxic N-terminal of gasdermins generated from caspases mediated cleavage of gasdermin proteins oligomerizes and forms pores across the cell membrane, leading to the release of proinflammatory cytokines such as interleukin-1β (IL-1β) and interleukin-18 (IL-18). Aberrant activation of pyroptosis has been implicated in the progression of many diseases including cancer and autoimmune, cardiovascular, and infectious diseases [15–17]. Recent studies have shown that the interactions between pyroptosis and autophagy play an important role in various physiological and pathological processes [15–20]. For example, autophagy inhibition upregulates galangin-induced pyroptosis in human glioblastoma multiforme cells and promotes pneumococcus-induced pyroptosis [21, 22]. However, the studies defining the molecular interactions between the pyroptosis, and autophagy pathways are very limited.

With a better understanding of the fundamental process of autophagy, its pathophysiological functions have begun to be appreciated in the female reproductive tract. For example, mice deficient in key autophagy genes such as genetic knockout of *Atg7* or *Becn1* result in primary ovarian insufficiency and reduced progesterone production [23, 24]. Similarly, recent studies from our group established the roles of three different autophagy-specific genes: ATG16L, FIP200/RB1CC1, or BECN1 in endometrial physiological processes, including receptivity and decidualization [25–27]. However, none of these proteins exhibited any discernible impact on oviduct function. Surprisingly, in this study, we revealed a critical role for Atg14 in maintaining proper oviduct function, specifically enabling the transport of embryos to the uterus-a function distinct from that of other autophagy-related proteins. Loss of ATG14 in the oviduct resulted in severe structural abnormalities, compromising its cellular integrity, ultimately leading to embryo retention and infertility.

Materials and methods

Animal care and use

All animal studies were approved by the Institutional Animal Care and Use Committee of Washington University School of Medicine, Saint Louis, MO, USA and Use Committee of Baylor College of Medicine, Houston, TX, USA. *Atg14* f/f mice were provided by gift from Dr. Shizuo Akira at the Department of Host Defense, Research Institute for Microbial Diseases (RIMD), Osaka University, and previously described [28]. Wild type Pr-cre mice were provided by Dr. John Lydon at Baylor College of Medicine, Houston and previously described [29]. $Atg14^{flox/flox}$ mice, in which exon 4 was flanked by loxp sites, were bred to progesterone receptor cre ($PR^{cre/+}$) mice to generate ($Atg14^{flox/flox}$; $PR^{cre/+}$ mice), hereafter referred to as *Atg14* cKO mice. Both control and conditional knockout females were generated by crossing females carrying homozygous $Atg14^{flox/flox}$ alleles with *Atg14* cKO males. *Foxj1-cre* mice were a generous gift from Dr. Michael J. Holtzman at Washington University St. Louis and previously described [30]. *Foxj1*/*Atg14* cKO mice were generated by crossing females carrying homozygous $Atg14^{f/f}$/$Foxj1^{f/f}$ females with $Atg14^{f/f}$/*Foxj1-cre* males. All mice were age-matched and on a C57BL/6 genetic background (The Jackson Laboratory, Bar Harbor, ME). Mice were genotyped by PCR analysis of genomic DNA isolated from tail clippings using the gene-specific primers listed in Supplementary Table 1.

Fertility analysis and timed mating

Female fertility was determined by mating cohorts of *Atg14* cKO experimental (n=6) and control *Atg14* f/f (n=4) females individually starting at 8 weeks of age with sexually mature males of proven fertility. Similarly, breeding trials were set up for *Foxj1/Atg14*-cre females (n=6) and *Foxj1*/*Atg14* control 8-week-old f/f females (n=6). The numbers of litters and pups were tracked over 6 months for each female. Pups per litter for each genotype are reported as mean ± SEM. For timed mating, the morning on which the copulatory plug was first observed was considered 1 dpc. To visualize implantation sites, mice received a tail vein injection of 50 µL of 1% Chicago Sky Blue dye (Sigma-Aldrich, St. Louis, MO, USA) at 5 dpc just before sacrifice.

Steroid hormone treatments

The hormonal profile of pregnancy at the time of implantation was done using a previously described experimental scheme [26]. Briefly, *Atg14* cKO and control females (8 weeks old) were bilaterally ovariectomized under ketamine anesthesia with buprenorphine-SR as an analgesic. Mice were allowed to rest for two weeks to dissipate all endogenous ovarian hormones. After the resting period, mice were injected with 100 ng of estrogen (E2; Sigma-Aldrich) dissolved in 100 µL of sesame oil on two consecutive days and then allowed to rest for two days. At this point, mice were randomly divided into three groups of five: Vehicle-treated (E2 priming) mice received four consecutive days of sesame oil injections; E2 group mice received three days of sesame oil injections followed by a single injection of 50 ng of E2 on the fourth day; The E2/P4 mice received 1 mg of progesterone (P4; Sigma-Aldrich) for three consecutive days followed by a single injection of 1 mg P4 plus 50 ng E2 on the fourth day. All hormones were delivered by subcutaneous injection in a 90:10 ratio of sesame oil: ethanol. Mice were euthanized 16 hours after the final hormone injection to collect the uteri. A small piece of tissue from one uterine horn was processed in 4% neutral buffered paraformaldehyde for histology, and the remaining tissue was snap-frozen and stored at −80°C.

Hormone Analysis

For serum hormone levels measurement, blood was collected from D4 pregnant mice before mice were sacrificed. Serum was separated from the blood by centrifugation and stored at −80°C before hormone analysis. Serum P4 and E2 levels were measured by using ELISA kits (Enzo life Sciences) according to the manufacturer's instructions.

Hematoxylin and eosin staining

Tissues were fixed in 4% paraformaldehyde, embedded in paraffin, and then sectioned (5 µm) with a microtome (Leica Biosystem, Wetzlar, Germany). Tissue sections were deparaffinized, rehydrated, and stained with Hematoxylin and Eosin (H&E) as described previously [31]. All the histology was performed on three sections from each tissue of individual mice, and one representative section image is shown in the respective figures.

Histological analysis

For histological analysis, the collected tissues (oviduct or uteri) were fixed in 4% paraformaldehyde, embedded in paraffin, and sectioned. Sections (5 µm) were immunostained (n=5 per group) as described previously [31]. Briefly, after deparaffinization, sections were rehydrated in an ethanol gradient and then boiled for 20 min. in citrate buffer (Vector Laboratories Inc., Newark, CA, USA) for antigen retrieval. Endogenous peroxidase activity was quenched with Bloxall (Vector Laboratories Inc.), and tissues were blocked with 2.5% goat serum in PBS for 1 hr (Vector Laboratories Inc.). After washing in PBS three times, tissue sections were incubated overnight at 4 °C in 2.5% goat serum containing the primary antibodies listed in Supplementary Table 2. Sections were incubated for 1 hr with biotinylated secondary antibody, washed, and incubated for 45 min with ABC reagent (Vector Laboratories Inc.). Color was developed with 3, 3'-diaminobenzidine (DAB) peroxidase substrate (Vector Laboratories Inc.), and sections were counter-stained with hematoxylin. Finally, sections were dehydrated and mounted in Permount histological mounting medium (Thermo Fisher Scientific, Waltham, MA, USA).

Transmission electron microscopy (TEM)

For ultrastructural analysis, oviducts were fixed in 2% paraformaldehyde/2.5% glutaraldehyde (Ted Pella Inc., Redding, CA) in 100 mM cacodylate buffer, pH 7.2 for 1 hr at room temperature and then overnight at 4°C. Samples were washed in cacodylate buffer and postfixed in 1% osmium tetroxide (Ted Pella Inc.) for 1 hr. Samples were then rinsed extensively in dH20 prior to en bloc

staining with 1% aqueous uranyl acetate (Ted Pella Inc.) for 1 hr. Following several rinses in dH20, samples were dehydrated in a graded series of ethanol and embedded in Eponate 12 resin (Ted Pella Inc.). For initial evaluation semithin sections (0.5 µm) were cut with a Leica Ultracut UCT7 ultramicrotome (Leica Microsystems Inc., Bannockburn, IL) and stained with toluidine blue. Sections of 95 nm were then cut and stained with uranyl acetate and lead citrate and viewed on a JEOL 1200 EX II transmission electron microscope (JEOL USA Inc., Peabody, MA). Images at magnifications of 3,000X to 30,000X were taken with an AMT 8-megapixel digital camera (Advanced Microscopy Techniques, Woburn, MA).

Immunofluorescence analysis

Formalin-fixed and paraffin-embedded sections were deparaffinized in xylene, rehydrated in an ethanol gradient, and boiled in a citrate buffer (Vector Laboratories Inc.) for antigen retrieval. After blocking with 2.5% goat serum in PBS (Vector laboratories) for 1 hr at room temperature, sections were incubated overnight at 4°C with primary antibodies (Supplementary Table 2) diluted in 2.5% normal goat serum. After washing with PBS, sections were incubated with Alexa Fluor 488-conjugated secondary antibodies (Life Technologies, Carlsbad, CA, USA) for 1 hr at room temperature, washed, and mounted with ProLong Gold Antifade Mountant with DAPI (Thermo Fisher Scientific). All Immunofluorescence images were obtained using a Zeiss LSM 880 confocal microscope (10x and 40x objective lens).

Fresh oviduct tissues from 8-week-old mice from control (n=3) and cKO (n=3) were collected and fixed in 4 % PFA at 4°C overnight. After that, oviducts were washed with PBS and cryoprotected using gradually increased sucrose concentrations in a row (15 and 30% w/v). 24 h later, oviducts were embedded in an OCT medium, frozen (−80 °C), and cryo-sectioned in the CM3050S Cryostat (Leica Biosystems, Germany). The cryosections were mounted on Superfrost plus glass slides (Fisher Scientific, Pittsburgh, PA) and stored at −80°C until used.

Cryo-sections were processed for immunofluorescence staining as described before [32]. Briefly, cryosections were blocked in 2.5% normal goat serum. After washing with PBS, sections were blocked with Mouse on Mouse (M.O.M.) IgG blocking reagent (M.O.M. Fluorescein Kit, Vector Laboratories, #FMK-2201) diluted in 1% BSA per the manufacturer's instructions. After blocking, sections were incubated overnight at 4°C with primary antibodies (Supplementary Table 2) diluted in 2.5% normal goat serum. Next day, following washing with PBS, sections were incubated with Alexa Fluor 488-conjugated secondary antibodies (Life Technologies, Carlsbad, CA, USA) for 1 hr at room temperature, washed, and mounted with ProLong Gold Antifade Mountant with DAPI (Thermo Fisher Scientific). All Immunofluorescence images were imaged using a Nikon Fluorescent microscope.

Western blotting

Protein lysates (40 µg per lane) from uteri or oviducts were loaded on a 4-15% SDS-PAGE gel (Bio-Rad, Hercules, CA, USA), separated in 1X Tris-Glycine Buffer (Bio-Rad), and transferred to PVDF membranes via a wet electro-blotting system (Bio-Rad), all according to the manufacturer's directions [33]. PVDF membranes were blocked for 1 hour in 5% non-fat milk in Tris-buffered saline containing 0.1% Tween-20 (TBS-T, Bio-Rad), then incubated overnight at 4 °C with antibodies listed in Supplementary Table 2 in 5% BSA in TBS-T. Blots were then probed with anti-Rabbit IgG conjugated with horseradish peroxidase (1:5000, Cell Signaling Technology, Danvers, MA, USA) in 5% BSA in TBS-T for 1 hr at room temperature. Signal was detected with the Pierce™ ECL Western Blotting Substrate (Millipore, Billerica, MA, USA), and blot images were collected with a Bio-Rad ChemiDoc imaging system.

RNA Isolation and Quantitative Real-Time RT-PCR Analysis

Tissues/cells were lysed in RNA lysis buffer, and total RNA was extracted with the Purelink RNA mini kit (Invitrogen, Carlsbad, CA, USA) according to the manufacturer's instructions. RNA was quantified with a Nano-Drop 2000 (Thermo Fisher Scientific). Then, 1 µg of RNA was reverse transcribed with the High-Capacity cDNA Reverse Transcription Kit (Thermo Fisher Scientific). The amplified cDNA was diluted to 10 ng/µL, and qRT-PCR was performed with primers listed in the Supplementary Table 1 and TaqMan 2X master mix (Applied Biosystems/Life Technologies, Grand Island, NY, USA) on a 7500 Fast Real-time PCR system (Applied Biosystems/Life Technologies). The delta-delta cycle threshold method was used to normalize expression to the reference gene 18S.

Treatment of mice with Polyphyllin VI

Polyphyllin VI (Selleck chemicals, Houston, TX, USA), a pharmacological agent that induces caspase-1-mediated pyroptosis, was used to study its effects on embryo transport in the oviduct [34]. Eight-week-old C57BL/6 mice were injected for three consecutive days starting from 1 dpc with Polyphyllin VI activator dissolved in 40% PEG-300 (15mg/kg body weight). Dimethyl sulfoxide with 40% PEG-300 was administered as a vehicle.

Statistics

A two-tailed paired student t-test was used to analyze data from experiments with two experimental groups and one-way ANOVA followed by Tukey's post hoc multiple range test was used for multiple comparisons. All data are presented as mean ±SEM. GraphPad Prism 9 software was used for all statistical analyses. Statistical tests, including p values, are reported in the corresponding figure legends or, when possible, directly on the data image. To ensure the reproducibility of our findings, experiments were replicated in a minimum of three independent samples, to demonstrate biological significance, and at least three independent times to ensure technical and experimental rigor and reproducibility.

Results

Conditional deletion of *Atg14* in the FRT results in infertility despite the normal ovarian function

To explore the role of *Atg14* in uterine function, we first determined its expression levels in uterus during early pregnancy (Day 1-7) in mice. We found distinct expression of ATG14 in all the uterine compartments (luminal epithelium, glands, and stroma) by day 1 of pregnancy, which disappeared by day 2 of pregnancy (**Fig. 1A**). However, the ATG14 expression in uterus reappeared by day 3 and persisted through the day 7 of pregnancy. The period from day 3 to day 7 is critical, as it is during this time when uterus begins to prepare for embryo implantation and undergoes decidualization process. Consistent with protein expression, similar *Atg14* expression at mRNA levels was noted in uteri from early pregnant mice (**Fig. 1B**). This analysis suggests a potential role for ATG14 protein in the uterine physiologic adaptations during early pregnancy. Thus, to study the role of ATG14 in uterine function, we generated a conditional knockout ($PR^{cre/+}$ /$Atg14^{flox/flox}$) mouse model by crossing *Atg14* flox/flox mice with mice expressing Cre recombinase under the control of progesterone receptor promoter ($PR^{cre/+}$). Histological examination of the uterus from adult females showed no gross morphological differences between *Atg14* cKO and control mice (Fig. S1A). Further, we did not find any overt defects in ovary as cKO mice had normal follicles and corpus luteum as like their corresponding controls (Fig. S1B). Analysis of transcript levels from the uterus, ovary, and liver showed that while *Atg14* levels were efficiently depleted in uteri from cKO mice the levels were unaltered in the ovary and liver

samples in control and cKO mice (**Fig. 1C**). Immunofluorescence analysis further confirmed the efficient deletion of ATG14 in all uterine compartments (epithelium and stroma) of cKO mice uteri compared to corresponding control groups (**Fig. 1D**).

Considering the effective ablation, a 6-month breeding study was performed mating virile wild-type male mice with adult *Atg14* cKO and control female mice. We found that *Atg14* cKO females did not deliver any litter during the 6-months trial period. However, the control female (*Atg14* flox/flox) mice delivered an average of ~7-8 pups per litter every month (**Table 1**) (**Fig. 1E**). These findings suggest an indispensable role of *Atg14* in female fertility with intact ovarian function.

Loss of *Atg14* results in impaired embryo implantation and uterine receptivity in mice

Based on the normal ovarian morphology, we posited that the infertility observed in females with *Atg14* cKO status could be attributed to compromised uterine functioning. Analysis of the implanting embryos at Day 5 of pregnancy showed no implantation sites in the uteri of *Atg14* cKO females, whereas ~8 to 9 implantation sites were seen in the uteri of control mice at 5 dpc (**Fig. 2A, left panel**). Whilst there was no embryo present in the uterine lumen of *Atg14* cKO mice, a fully attached embryo encapsulated by the luminal uterine epithelium, was seen in control mice uteri (**Fig. 2A, middle panel**). Additionally, MUC1, a receptive marker expression persisted in the luminal epithelium of cKO mice uteri at 5 dpc as well as 4 dpc (**Fig. 2A, right panel**, **Fig. 2C**). The process of successful embryo attachment and implantation within the uterus necessitates a transition from a non-receptive to a receptive state, a transformation orchestrated under the regulated influence of steroid hormones. Thus, the effects of *Atg14* loss on uterine responsiveness to steroid hormones E2 and P4 were characterized. We performed an established hormone-induced uterine receptivity experiment, which involved ordered and co-stimulatory actions of E2 and P4 leading to the initiation of a receptive phase [35]. In response to E2 treatment, uteri from both *Atg14* control and cKO mice showed similar proliferation as evidenced by Ki-67 staining (**Fig. 2B, middle panel**). Following the co-stimulation with E2+P4 treatment, epithelial proliferation was inhibited with concomitant induction of stromal cell proliferation in control mice uteri indicating fully receptive uteri (**Fig. 2B**). Interestingly, cKO mice uteri failed to elicit sub-epithelial stromal cell proliferation and showed intact P4-driven inhibition of epithelial proliferation. Consistently, uteri from *Atg14* cKO mice at 4 dpc showed a reduced number of proliferating stromal cells (**Fig. 2D**). The absence of significant changes in E2-induced targets, such as *Lif*, *Mcm2*, *Ccnd1*, and *Fgf18*, at 4 dpc (**Fig. 2E**) supports our conclusion that ATG14 is required for P4-mediated but not for E2-mediated actions during uterine receptivity. Moreover, the normal serum levels of E2 and P4 at D4 of pregnancy rule out any hormonal imbalances, strongly suggesting that the observed phenotype is primarily due to the uterine-specific loss of *Atg14* (**Fig. 2F**).

Atg14 is required for maintaining oviductal cell structural integrity and embryo transport

Given that *Atg14* cKO mice had impaired embryo implantation, we wondered whether embryos are reaching the uterus timely through the oviduct. To determine this, we flushed embryos from both the control and cKO mice uteri on day 4 of pregnancy. Interestingly, in cKO mice, we could retrieve only 1-2% of embryos from their uteri, whereas in control mice, 100% of well-developed blastocysts were retrieved from their uteri (**Fig. 3A & B**). To ensure the timely transport of all embryos from the oviducts to the uteri, we also flushed oviducts from both control and cKO mice. As expected, in the control mice oviduct flushing, we could not recover any embryos or blastocysts, indicating their precise and timely transport to the uterus. Unexpectedly, oviduct flushing from cKO mice resulted in the retrieval of approximately 80-90% of blastocysts,

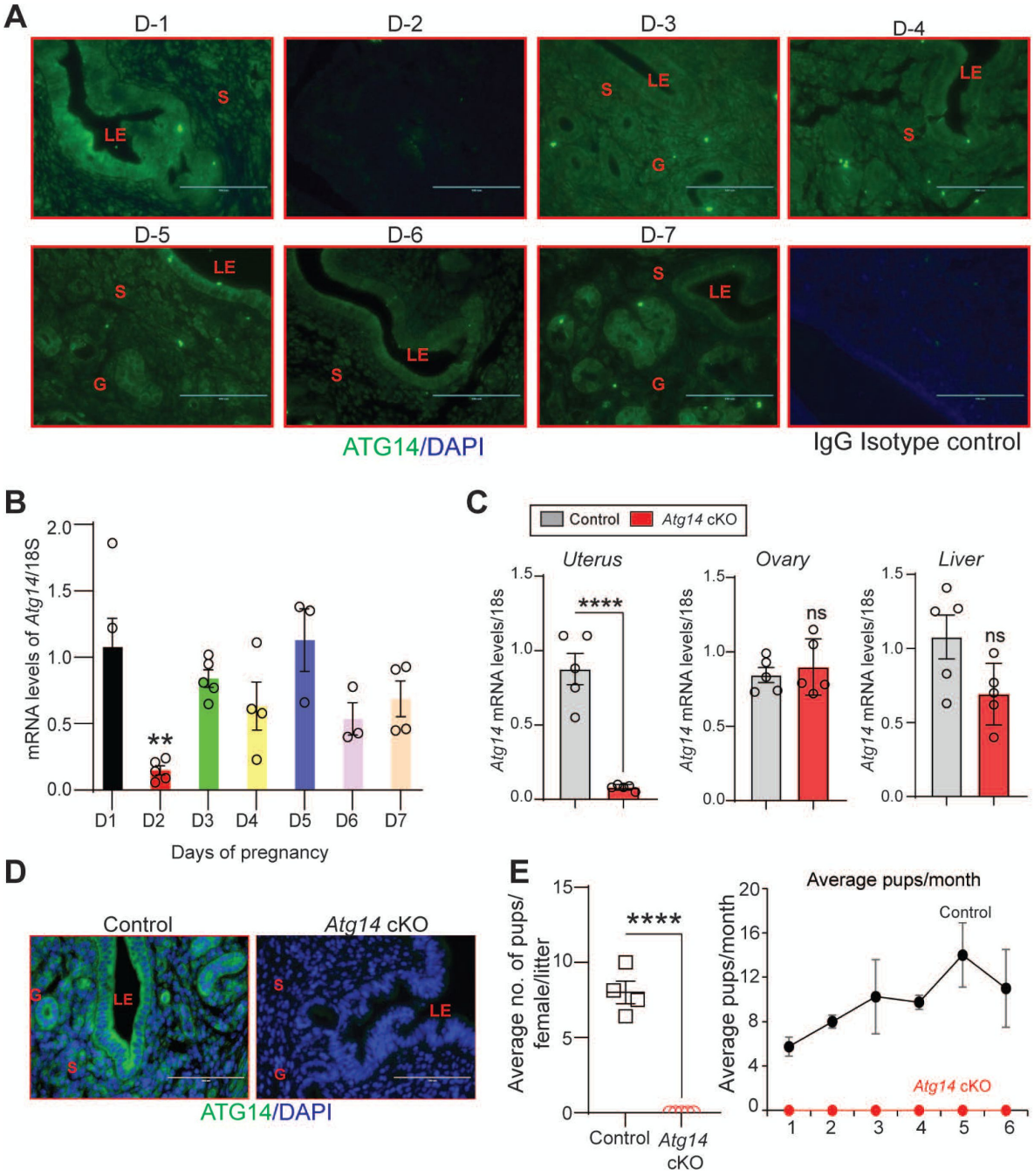

Figure 1

***Atg14* loss in the FRT results in infertility.**

(**A**) Representative immunofluorescent images of uteri from pregnant mice (n=3) at the indicated days of pregnancy stained with an ATG14-specific antibody (green). LE: luminal epithelium, G: glands, S: stroma, Scale bar: 100 µm. Rabbit IgG was used as an isotype control for staining. (**B**) Relative transcript levels of *Atg14* mRNA in uteri from pregnant mice (n=3-5) at indicated days of pregnancy. mRNA levels are normalized to levels of 18S m-RNA. Data are presented as mean ±SEM; **P<0.01, P>0.05, ns=non-significant. (**C**) Relative mRNA levels of *Atg14* in 8-week-old virgin control and cKO mice uteri, ovary, and liver (n=5). mRNA levels are normalized to levels of 18S mRNA. Data are presented as mean ±SEM; ***P<0.001, P>0.05, ns=non-significant. (**D**) Representative immunofluorescent images of ATG14 expression in different uterine compartments in control (n=5) and *Atg14* cKO mice (n=5). LE: luminal epithelium, G: glands, S: stroma. (**E**) (*left panel*) Relative number of pups/female/litter and (*right panel*) and relative number of total pups/months of *Atg14* control (n=4) and cKO mice (n=5) sacrificed after the breeding trial. Data are presented as mean ±SEM; ***P<0.001; P>0.05, ns=non-significant.

Table 1

Six-month breeding trial of *Atg14* control and cKO females with wild-type males

Genotype	Females	Pups	Pups/female	Litters	Pups/litter
Control	n=4	223	55.75±7.32	28	7.96±0.37
Atg14 cKO	n=6	0	0	0	0

Figure 2

Atg14 is critical for embryo implantation, and uterine receptivity.

(**A**) Gross images of 5.0 dpc uteri of control (n=5) and *Atg14* cKO mice (n=5) injected with Chicago Sky Blue dye to visualize implantation sites (denoted by black arrows) (*left panel*). H&E-stained cross-sections (4X & 40X) of 5.0 dpc uteri of control (n=5) and *Atg14* cKO (n=5) mice to visualize embryo implantation (*Middle panel*). The asterisk denotes the embryo. Immunofluorescence analysis of uterine tissues from control (n=5) and *Atg14* cKO mice (n=5), stained with MUC1 and KRT8 (*right panel*). LE: luminal epithelium, G: glands, S: stroma. (**B**) Representative immunofluorescence images of uteri from control (n=5) and *Atg14* cKO mice (n=5) stained for Ki-67 following Oil or E2 or E2+P4 treatment (n=5 mice/group); scale bar: 100 µm. LE: luminal epithelium, G: glands, S: stroma. (**C**) Immunofluorescence analysis of KRT8 (green), MUC1 (Red), and (**D**) Ki-67 (red) in the uteri of 4 dpc control and *Atg14* cKO mice; scale bars, 100 µm. (**E**) Relative transcript levels of *Lif*, *Mcm2*, *Ccnd1,* and *Fgf18* in control and cKO uteri at 4dpc. mRNA levels are normalized to levels of 18S m-RNA. Data are presented as mean ±SEM; ns=non-significant. (**F**) Levels of steroid hormones estradiol and progesterone from serum collected during euthanasia of 4 dpc control or cKO mice.

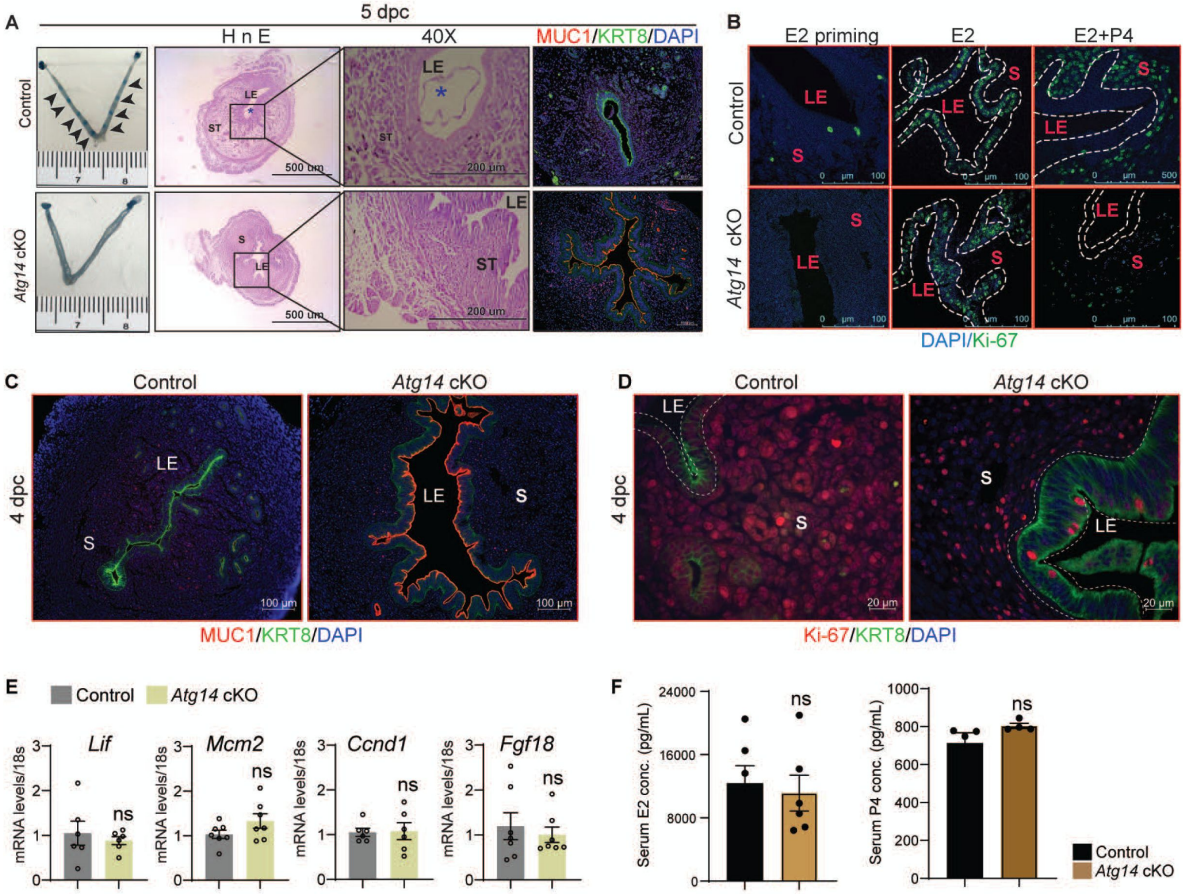

suggesting their potential entrapment within the oviducts, impeding their transit to the uterus (**Fig. 3A & B**). At 4 dpc, there was no significant difference in the average number of blastocysts, morula, or non-viable or retrieved from *Atg14* control uteri and cKO oviducts (Fig. S4A). However, we noted that the percentage of developmentally delayed embryos appeared to be higher in *Atg14* cKO oviducts compared to the embryos retrieved from control uteri (**Fig. 3C**). The histological analysis further confirmed an entrapped embryo in the ampulla of *Atg14* cKO at 4 dpc as shown in **Fig. 3D**. Given the embryo retention phenotype in oviduct, we sought to determine if ATG14 is expressed in this region. Consistent with previous studies reporting PR-cre activity in the isthmus [8, 29], we found a significant depletion of ATG14 in the isthmus compared to the ampulla (Fig. S2A). Further, the increased p62 and LC3B expression in cKO oviducts suggests that the observed embryo retention phenotype might be attributed to the loss of ATG14-dependent autophagy in cKO oviducts (Fig. S2B).

Similarly, when we super-ovulated the mice and looked for the embryos on day 4 of pregnancy, we could recover ~20-25 embryos from the cKO mice oviducts compared to only 4-5 embryos that were able to reach the uterus. In comparison, in control mice, 90% of embryos were able to complete their pre-destined and timely transport to the uterus (**Fig. 3E**), except 1-2% of unfertilized embryos, which remained in their oviducts.

To understand the underlying cause for retained embryos in cKO mice oviducts, we performed histology analysis and determined the structural morphology of their oviducts. The cKO mice oviduct lining shows marked eosinophilic cytoplasmic change akin to decidualization in human oviducts. Some of the cells showed degenerative changes with cytoplasmic vacuolization and nuclear pyknosis, loss of nuclear polarity, and loss of distinct cell borders giving an appearance of fusion of cells (**Fig. 3F**). The marked cytologic enlargement appears to cause luminal obliteration or narrowing resulting in a completely unorganized, obstructed, and narrow lumen, thereby, hampering the path of embryos to reach the uterus as evident from an entrapped embryo shown in **Fig. 3D**. Further, epithelial (cytokeratin KRT8-positive) and myosalpinx (α-smooth muscle active [SMA]-positive,) marker analysis revealed completely distorted epithelial structures (in terms of loss of epithelial cell integrity) with no overt defects in the muscle organization in oviducts of cKO mice (**Fig. 3F, lower panel**). Notably, the ampullary region from cKO oviducts seems to be normal with intact epithelial and smooth muscle structures as evident from KRT8 and SMA staining (**Fig. 3F, upper panel**).

Selective loss of *Atg14* in oviduct cilia is dispensable for female fertility

The oviduct epithelium primarily consists of two types of cells: ciliated and secretory (non-ciliated) cells. Ciliated cells play a role in embryo and oocyte transport by means of ciliary beat, and non-ciliated/secretory cells produce an oviductal fluid that is rich in amino acids and various molecules, thereby providing an optimal micro-environment for sperm capacitation, fertilization, embryonic survival, and development [36]. Therefore, we determined whether oviducts from cKO mice possess normal ciliated and secretory cell composition. To do so, we examined the expression of various markers, including acetylated-α-tubulin (cilia marker), FOXJ1 (ciliogenesis markers), and PAX8 (non-ciliated/ secretory cell marker) in control and cKO oviducts. As shown in **Fig. 4A**, while we observed normal ciliary structures in the ampulla of both control and cKO oviducts, there was a substantial loss of the ciliary epithelial cells (indicated by fewer α-tubulin and FOXJ1-positive cells) (**Fig. 4B, left panel** and Fig. S3) as well as secretory cells (indicated by fewer PAX-8 positive cells) in the isthmus of cKO oviducts (**Fig. 4B, right panel**).

Given the importance of cilia in embryo transport, we wondered whether the loss of *Atg14* in oviduct cilia has any impact on embryo transport. To address this, we generated a *Foxj1*-cre/+; *Atg14* f/f mouse model, wherein *Atg14* will be ablated only in ciliary epithelial cells. We observed

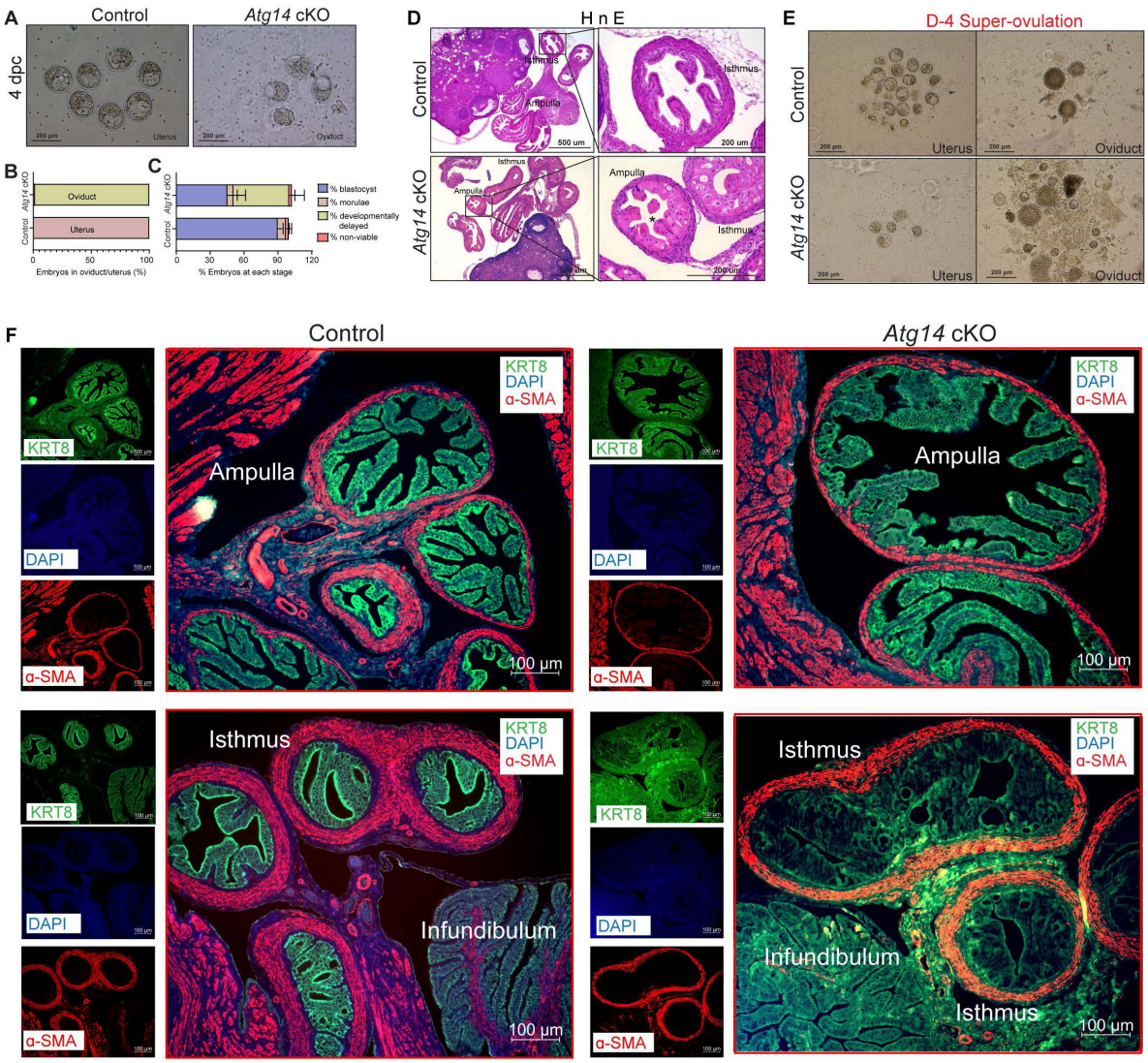

Figure 3

Atg14 is critical for embryo transport in oviduct.

(**A**) Representative images (*upper panel*) and (**B**) Percentage of embryos (*lower panel*) collected at 4 dpc from the uteri or the oviducts of control (n=6) or *Atg14* cKO mice (n=6-8). (**C**) Percentage of blastocysts, morulae, developmentally delayed or nonviable embryos collected from *Atg14* control mice uteri and Atg14 cKO mice oviducts at 4 dpc. (**D**) Histological analysis using H&E staining of the ampullary and isthmic region of the oviduct from control and *Atg14* cKO female mice at 4 dpc (n=3 mice/genotype). (**E**) Embryos retrieved from the oviduct and uterus of super-ovulated *Atg14* control or cKO mice at 4 dpc (n=3 mice/genotype). (**F**) Immunofluorescence analysis of KRT8 (green), and α-SMA (Red), in the oviduct of 4 dpc control (n=5) and *Atg14* cKO mice (n=5) ampulla (*upper panel*) and isthmus (*lower panel*).

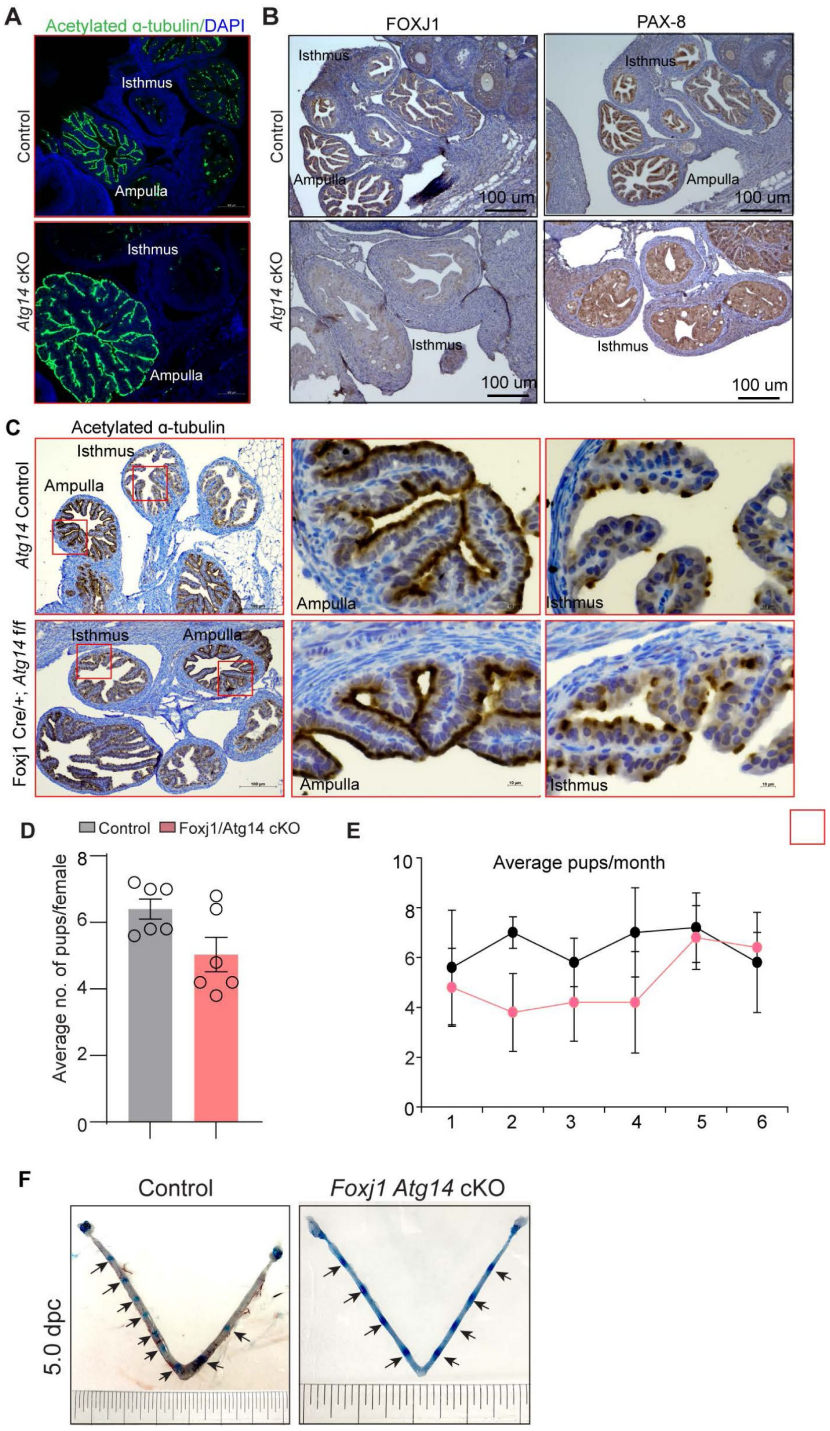

Figure 4

Atg14 loss in oviduct cilia is dispensable for embryo transport.

(A) Immunofluorescence analysis of acetylated α-tubulin (green), and DAPI (blue) in oviduct of 4 dpc control (n=5) and *Atg14* cKO mice (n=5). (**B**) Immunohistochemical analysis of FOXJ1 and PAX8 at 4 dpc (n=5). (**C**) Immunohistochemical analysis of acetylated α-tubulin in 8-week-old control (n=5) and *Foxj1*/*Atg14* cKO mice (n=5). Images are taken at 6X and 40X. Scale bar: 100μm and 10 μm. (**D & E**) Relative number of pups/females/litter and relative number of total pups/months of control (n=5) and *Foxj1*/*Atg14* cKO mice (n=5) sacrificed after the breeding trial. Data are presented as mean ± SEM; P>0.05, ns=non-significant. (**F**) Gross images of 5.0 dpc uteri of control (n=3) and *Foxj1/Atg14 cKO mice* (n=3) injected with Chicago Sky Blue dye to visualize implantation sites (denoted by black arrows).

that ciliated epithelial cells that were positive for acetylated α-tubulin staining did not appear to be different in Foxj1$^{Cre/+}$:*Atg14* f/f mice oviduct compared to controls suggesting normal ciliogenesis in Foxj1$^{Cre/+}$; *Atg14* f/f mice (**Fig. 4C**).

The 6-month breeding trial revealed that loss of *Atg14* in oviductal cilia had no impact on fertility (**Table 2**, **Fig. 4D & E**). Consistently, D5 implantation study analysis showed ~7-8 visible embryo implantation sites in *Foxj1/Atg14* cKO mice like their corresponding controls suggesting that embryos were able to make their way to the uterus in a timely manner and undergo implantation despite the ablation of *Atg14* in the oviduct ciliary epithelial cells (**Fig. 4F**). These findings suggest that ciliary expression of *Atg14* is dispensable for embryo transport.

ATG14 maintains mitochondria integrity and prevents unscheduled pyroptosis activation in the oviduct to enable embryo transport

To gain more insights into structural defects, we performed TEM analysis on oviducts collected from both control and cKO females on day 4 of pregnancy. Interestingly, oviducts from cKO females had numerous altered mitochondrial structures with abnormally enlarged mitochondria and a less dense matrix compared to control oviducts that had small and compact mitochondria with tight cristae and a dense matrix (**Fig. 5A**). Corroborating and extending those findings, we observed marked reductions of mitochondria network (as defined by TOMM20 staining) in the sub-nuclear region of oviducts from *Atg14* cKO mice compared to more densely packed mitochondrial network in the sub-nuclear region of control ones (**Fig. 5B**). Further co-localization study analysis revealed a uniform co-localization of Cytochrome C with the TOM20 positive mitochondrial network in control oviducts reflecting the intact mitochondrial integrity (**Fig. 5B**). In contrast, in *Atg14* cKO oviducts, cells with disrupted mitochondrial networks exhibited increased cytosolic leakage of Cytochrome C (**Fig. 5B**). Additionally, analysis of various mitochondrial functional and architecture markers (*Cox4i2*, *Pink1*, *Opa1*, and *Drp1* showed reduced expression in *Atg14* cKO compared to controls (**Fig. 5C**).

Having identified the cellular mechanisms of Atg14, we aimed to delineate the underlying molecular mechanisms associated with Atg14 function in the oviduct. Since we found mitochondrial defects with ATG14 loss and altered mitochondrial structures have been linked to the activation of pyroptosis, we determined if ATG14 regulates pyroptosis in oviduct [37–39]. First, we assessed the key primary executors of the pyroptosis pathway, Gasdermin D (GSDMD), and caspase-1. Immunofluorescence analysis revealed a remarkable upregulation in GSDMD and caspase-1 expression in the cKO oviducts compared to controls (**Fig. 5D & E**). However, histological analysis of uterus and ovary showed no induction in GSDMD expression compared to their corresponding controls (**Fig. 5F**). Western blot analysis further confirmed elevated expression of caspase-1 and GSDMD in cKO oviducts in comparison to control oviducts as shown in **Fig. 5G**. Additionally, the qPCR analysis demonstrated elevated levels of inflammatory markers, such as *Tnf-α* and *Cxcr3* in cKO oviducts compared to control ones (**Fig. 5H**). Based on these findings, we posit that Atg14 plays a crucial role in regulating the pyroptotic pathway by preserving the mitochondrial structural and functional integrity, and activation of pyroptosis owing to loss of ATG14 within the oviduct.

To substantiate the notion, we also evaluated the impact of unscheduled activation of pyroptosis on embryo transport. To test this, we employed a pyroptosis inducer, Polyphyllin VI, and chose the optimal dose based on the established studies [34]. Wild-type females were mated with virile males and following the plug detection treated with Polyphyllin VI for three consecutive days from 1 to 4 dpc (**Fig. 5E**). We chose to treat to 1 to 4 dpc for treatment to activate unwarranted pyroptosis in oviduct during the embryo transport. Following the treatments, the oviducts, and uteri from both vehicle-treated and Polyphyllin VI-treated were flushed. We found that pregnant

Genotype	Females	Pups	Pups/female	Litters	Pups/litter
Control	n=5	192	38.4±1.29	26	9.1±1.29
Foxj1/Atg14 cKO	n=5	151	30.2±1.46	24	7.6±1.46

Table 2

Six-month breeding trial of *Foxj1*/*Atg14* control and cKO females with wild-type males

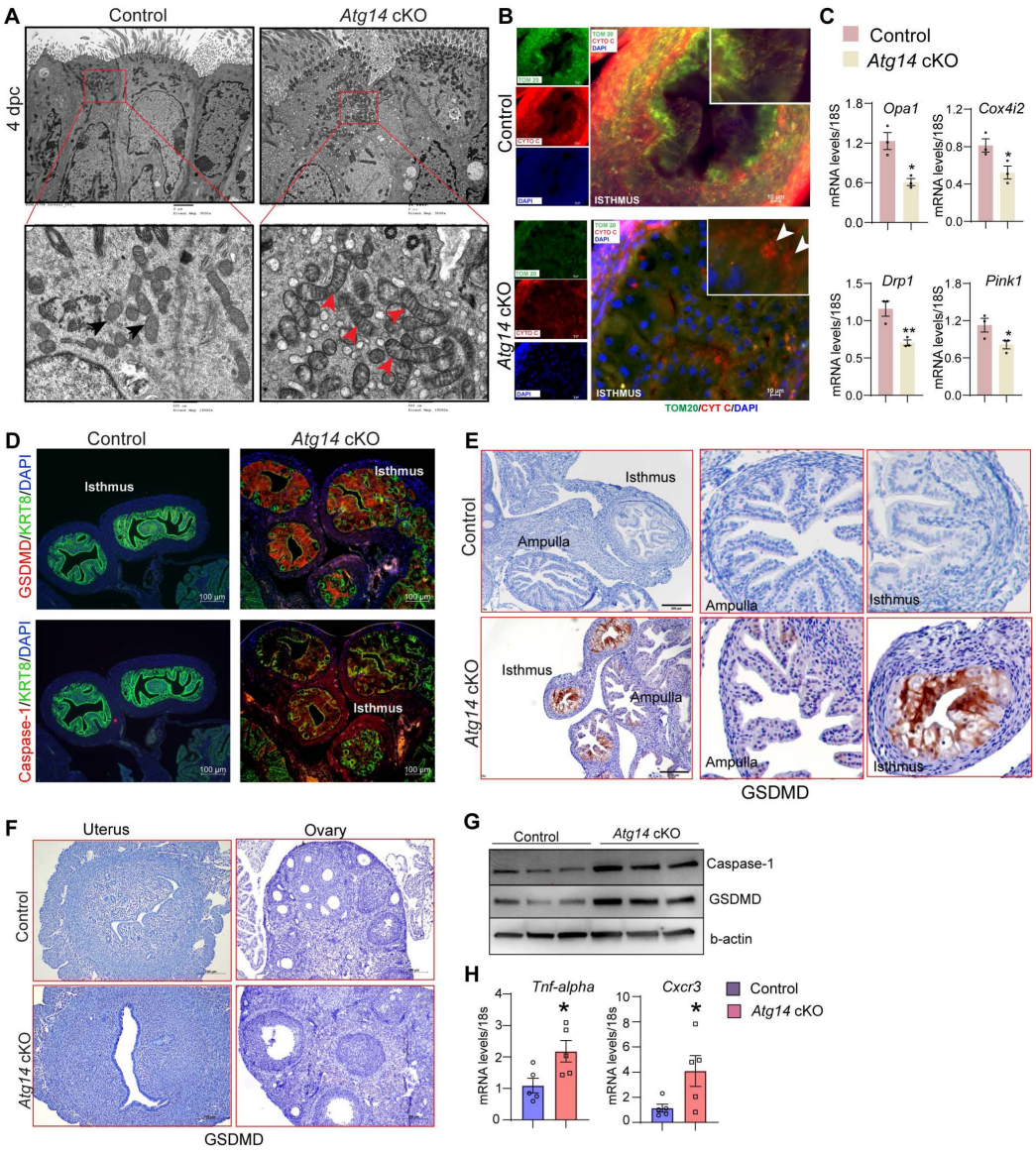

Figure 5

>ATG14 facilitates embryo transport in the oviduct by preserving mitochondrial integrity and inhibiting the activation of pyroptosis.

(**A**) Transmission electron microscopy of oviducts at 4 dpc from control (n=3) and *Atg14* cKO (n=3). Black arrowheads in control oviducts show small, compact mitochondria with tight cristae. Red arrowheads in cKO oviducts show abnormally enlarged mitochondria with loose cristae. (**B**) Immunofluorescence analysis of TOM20 (green) and Cytochrome C (red) in *Atg14* control and cKO oviducts cryo-sections. The inset shows the zoomed image of the selected area from control and cKO oviducts, Arrowheads in cKO inset oviduct section show the leaked cytochrome C in the cytoplasm. Tissues were counterstained with DAPI (blue) to visualize nuclei; scale bars, 10 µm. (**C**) Relative transcript levels of *Opa1*, *Cox4i2*, *Drp1,* and Pink1 in oviduct tissues. Data are presented as mean ±SEM. *P<0.05; **P<0.01 compared with controls. 18S was used as an internal control (**D**) Immunofluorescence analysis of GSDMD (red) + KRT8 (green), Caspase-1 (red) + KRT8 (green) in oviducts of adult control (n=5), and *Atg14* cKO mice (n=5). Tissues were counterstained with DAPI (blue) to visualize nuclei; scale bars, 100 µm. (**E**) Immunohistochemical analysis of GSDMD expression in adult oviduct tissues (*left panel*). The middle and -right panels show the zoom-in images to show the relative GSDMD expression in the ampulla and isthmus section from control and cKO oviducts. (**F**) Immunohistochemical analysis of GSDMD expression in adult uterus and ovary tissues (**G**) Western blotting to show protein levels of Caspase-1, and GSDMD in oviduct tissues. β-actin is used as a loading control. (**H**) Relative transcript levels of *Tnf-α* and *Cxcr3* in oviduct tissues. Data are presented as mean ±SEM. *P<0.05; **P<0.01; ***P<0.001 compared with controls. 18S was used as an internal control.

females treated with Polyphyllin VI showed ~50% embryo retention in the oviduct, whereas in the vehicle-treated group, no embryos were retained in the oviduct (**Fig. 6A-C**). Further analysis of embryos retrieved from Polyphyllin-treated oviducts showed more percentage of developmentally delayed and non-viable embryos compared to embryos recovered from control uteri (**Fig. 6D**). The average number of embryos recovered from polyphyllin- and vehicle-treated mice was not significantly different (Fig. S4B). Histological analysis showed a marked induction in GSDMD expression compared to vehicle-treated mice oviducts (**Fig. 6E**). However, precisely activating the unscheduled pyroptosis during the critical period of embryo transport is technically challenging. Nonetheless, our findings provide evidence that unscheduled pyroptosis adversely affects embryo transport through the oviduct. Taken together, these results demonstrate that *Atg14* safeguards pyroptosis activation in the oviduct and allows the smooth transport of embryos to the uterus (**Fig. 6F**).

Discussion

In this study, we delineated the essential role of ATG14 in maintaining the structural integrity of the oviduct by preventing pyroptosis, which enables smooth embryo transit during early pregnancy. Specifically, we dissected the tissue-specific functions of ATG14 in the FRT using Cre driver mice targeting the female reproductive tract. Given that PR-Cre expresses postnatally in different tissues of FRT such as corpus luteum, oviducts, and different cellular compartments (epithelial, stromal, and myometrium) of uteri [29], we found that conditional ablation of ATG14-mediated functions in FRT resulted in infertility owing to hampered transport of embryos from the oviduct. Additionally, *Atg14* loss in uteri causes impaired embryo implantation and receptivity. Its ablation in the oviduct might lead to the activation of pyroptosis, an inflammatory-associated apoptosis pathway that causes the retention of embryos in the oviduct and prevents their timely transport to the uterus. However, the ovarian-specific functions were found to be unaffected despite the loss of *Atg14* in the corpus luteum.

The human endometrium is a complex dynamic tissue that undergoes sequential phases of proliferation and differentiation to support embryo implantation during the conceptive. However, in the absence of an implanting embryo, the endometrium sheds (menstruation) and initiates the regeneration process [40]. Previous reports indicated that autophagy is modulated in the human endometrium during the menstrual cycle. For example, autophagy is altered during the proliferative and secretory phases of the menstrual cycle with its highest activity occurring during the secretory phase when the stroma is decidualized [41]. Similarly, the level of autophagy was higher in postmenopausal human uterine epithelial cells compared to premenopausal uterine epithelial cells indicating the onset of autophagy upon estrogen deprivation [42]. Although all these studies reported that autophagy is hormonally regulated, however, the role of autophagy-specific proteins in the endometrium was not established till our group's recent reports. Specifically, studies from our group reported the role of three different autophagy-associated proteins: FIP200 [25], ATG16L [27], and BECLIN-1 in uterine functions [26]. Conditional ablation of *Fip200* and *Atg16l* in the uterus displayed fertility defects owing to impaired implantation, uterine receptivity, and decidualization defects. On the contrary, loss of *Beclin1* in the uterus caused progressive loss of endometrial progenitor stem cells resulting in severe uterine developmental defects and rendering the mice infertile [26]. Although the autophagy-related proteins we studied so far influenced uterine functions, [25–27], we found a distinct role for ATG14 in both the uterine and oviduct-specific functions. It is intriguing to note that the absence of ATG14 did not affect the tissue integrity of the uterus. However, the severe structural abnormalities in the oviduct due to *Atg14* ablation unearthed a unique function of Atg14 in maintaining oviduct homeostasis. This distinctive role of ATG14, unlike other autophagy proteins, might be due to its pivotal role in the assembly of PtdIns3K complexes which is not the case for

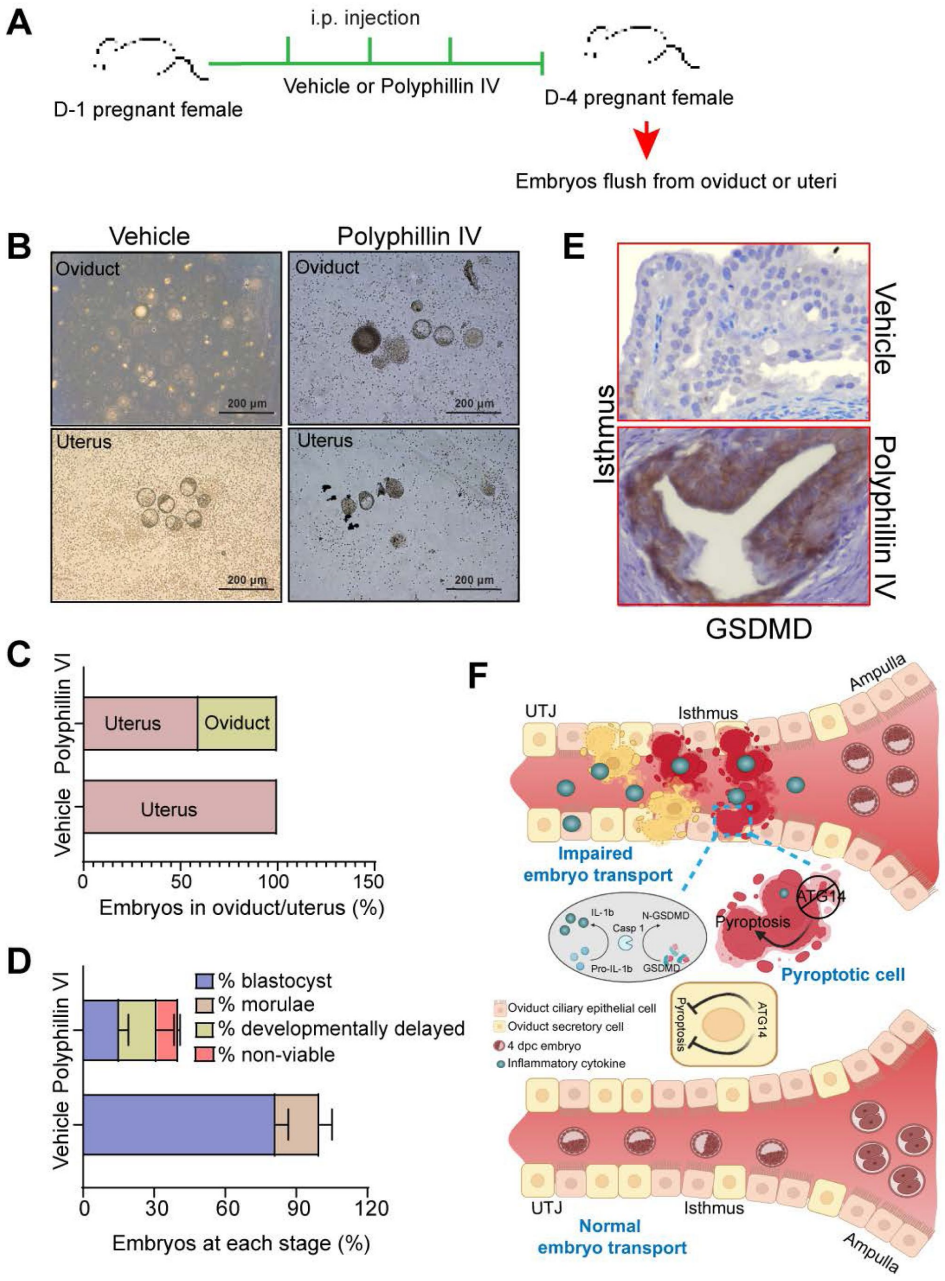

Figure 6

Pharmacological activation of pyroptosis in the oviduct inhibits embryo transport.

(**A**) Experimental strategy for pyroptosis activation in pregnant female mice (**B**) Embryos flushed from the vehicle (n=3) or polyphyllin VI treated (n=3) D-4 pregnant females. (**C**) Percentage of embryos recovered from oviducts or uteri. (**D**) Percentage of blastocysts, morulae, developmentally delayed or nonviable embryos collected from vehicle or Polyphyllin IV oviducts at 4 dpc. (**E**) Immunohistochemistry to show GSDMD expression in the isthmus section of polyphyllin IV-treated and vehicle-treated mice. 40X objective, Scale bar: 5 µm. (**F**) Graphical illustration to show embryo transport and pyroptosis regulation in the oviduct.

either FIP200 or ATG16L [40, 43, 44]. Nevertheless, understanding the specific contributions of each core autophagy protein in reproductive tract functions is necessary which requires substantial efforts.

The retention of preimplantation embryos in the oviduct has been established as a significant contributor to implantation failures, presenting challenges to the overall reproductive health of women [8–10]. Embryo transport in the oviduct is known to be controlled primarily by two major physiological responses: ciliary activity and muscle contractility. In our study, a dramatic decrease in the number of Foxj1^{+ve} ciliary epithelial cells and Pax-8^{+ve} secretory cells in *Atg14* cKO mice implied cell-type specific actions for ATG14 in the oviduct. Interestingly, the specific ablation of *Atg14* in Foxj1+ve ciliary epithelial cells of the oviduct does not appear to impact fertility. This suggests that the absence of ATG14 within ciliary cells does not impact the process of embryo transport. Although unexpected, this is consistent with other reports that have demonstrated the dispensability of cilia for embryo transport in the oviduct [8, 9].

Pyroptosis is a highly inflammatory form of programmed cell death, characterized by cell swelling, flattening of the cytoplasm, and large bubbles-like protrusions on the plasma membrane [45–47]. Several recent studies found a link between autophagy and pyroptosis [48]. *In vivo* studies also found that mice lacking the autophagy genes *Atg14*, *Fip200*, *Atg5*, or *Atg7* in myeloid cells had more pronounced lung inflammation [49]. In our study, cellular swelling, and fused membranous structures (a unique feature of activation of pyroptosis) observed in the oviductal epithelial folds from *Atg14* cKO mice. This aberrant activation of the pyroptosis pathway due to loss of *Atg14* appears to adversely affect the oviduct cellular structural integrity. These findings have implications beyond the oviduct, as autophagy can modulate the inflammatory signaling pathway through different avenues. For example, first, autophagy prevents mitochondrial reactive oxygen species release that can activate the inflammasome by inhibiting IL1-β and IL18 production through the digestion of dysfunctional mitochondria [50]. Second, autophagy is capable of targeting inflammasome complexes for degradation, which prevents the cleavage of pro-IL-1β and pro-IL-18 into biologically active forms. Finally, autophagy machinery further regulates IL-1β levels by engulfing and degrading pro-IL-1β proteins [50]. In our study, accumulation of abnormally enlarged and dysfunctional mitochondria in the absence of ATG14 in the oviduct clearly suggests the induction of severe inflammatory conditions hampering the embryo transit through the oviduct. These findings are further substantiated by the upregulation of pivotal mediators of the pyroptosis program, including GSDMD and caspase-1, in *Atg14* cKO mice. Notably, the induction of pyroptosis in the absence of ATG14 is specifically localized to the oviducts, with no parallel activation detected in either the ovary or uterus. One potential reason for this observed phenomenon could be the oviduct's unique molecular signatures that get activated in response to the presence of gametes. A recent study by Finnerty et al. (2024) reported that sperm induce pro-inflammatory conditions in the oviduct, which are preceded by an anti-inflammatory response triggered by the presence of embryos [51]. The persistent activation of inflammatory or pyroptotic conditions following the loss of Atg14 suggests that Atg14 may be a critical autophagy protein responsible for suppressing pyroptosis in the oviduct. Moreover, understanding the complex rheostat between the ATG14 and inflammation regulatory axis is highly intriguing and will necessitate future studies employing sophisticated models, such as combined knockout mice where ATG14 is deleted alongside key inflammatory regulators (e.g., NLRP3, GSDMD, or CASPASE-1).

In this report, we revealed tissue-specific roles of ATG14 in governing oviductal transport, and uterine receptivity which are necessary for embryo implantation and pregnancy establishment. Of mechanistic insights, we delineated a novel function of ATG14 as a negative regulator of pyroptosis, which is vital for proper embryo transport in the oviduct (**Fig. 6F**). Thus, this study not only sheds light on the involvement of autophagy in oviductal embryo transport but also

underscores the importance of autophagy in preserving the oviduct tissue integrity. Such insights hold promise for advancing our understanding of gynecological pathologies associated with the oviduct including tubal pregnancies.

Acknowledgements

We thank Goutham Davuluri, and Ashirbad Guria from our group for the technical assistance. We thank Dr. Robert Lawrence (senior editor at Baylor College of Medicine) for assistance with manuscript editing. We thank WashU Molecular Microbiology Imaging Facility for assisting us with transmission electron microscopy. This work was funded, in part, by the National Institutes of Health/National Institute of Child Health and Human Development (grants R01HD102680, R01HD104813, and R01HD065435) to RK, R01 HD-042311 to JPL, and in part by National Institutes of Health/National Heart, Lung, and Blood Institute (grant R35HL145242) to MJH.

Additional information

Authors' roles

PP and RK designed experiments, conducted most of the studies, analyzed the data, and wrote the manuscript. AKO, VKM, and MNR, conducted some of the experiments. MJH, JL, SA, YZ, and KHM, provided critical reagents for the study. RM helped us with oviduct pathology phenotype analysis. RK conceived the project, supervised the work, and wrote the manuscript. All authors critically reviewed the manuscript.

Conflict of Interest

The authors have declared that no conflict of interest exists.

Non-standard Abbreviations

- WT: Wild Type
- HESCs: Human Endometrial stromal cells
- dpc: Days post coitum
- E2: Estrogen
- P4: Progesterone
- VPS 15: Vacuolar sorting protein 15
- cKO: Conditional knockout
- FRT: Female reproductive tract
- GSDMD: Gasdermin D

References

1. Wang H., Dey S.K. (2006) **Roadmap to embryo implantation: clues from mouse models** *Nat Rev Genet* **7**:185–99

2. Ford M.J., et al. (2021) **Oviduct epithelial cells constitute two developmentally distinct lineages that are spatially separated along the distal-proximal axis** *Cell Rep* **36**

3. McKey J., et al. (2022) **Integration of mouse ovary morphogenesis with developmental dynamics of the oviduct, ovarian ligaments, and rete ovarii** *Elife* **11**

4. Harwalkar K., et al. (2021) **Anatomical and cellular heterogeneity in the mouse oviduct-its potential roles in reproduction and preimplantation developmentdagger** *Biol Reprod* **104**:1249–1261

5. Dirksen E.R., Satir P. (1972) **Ciliary activity in the mouse oviduct as studied by transmission and scanning electron microscopy** *Tissue Cell* **4**:389–403

6. Li S., et al. (2017) **Estrogen receptor alpha is required for oviductal transport of embryos** *FASEB J* **31**:1595–1607

7. Jiang R., et al. (2022) **CDC42 governs normal oviduct multiciliogenesis through activating AKT to ensure timely embryo transport** *Cell Death Dis* **13**

8. Herrera G.G.B., et al. (2020) **Oviductal Retention of Embryos in Female Mice Lacking Estrogen Receptor alpha in the Isthmus and the Uterus** *Endocrinology* **161**

9. Wang H., et al. (2004) **Aberrant cannabinoid signaling impairs oviductal transport of embryos** *Nat Med* **10**:1074–80

10. Qian J., et al. (2018) **Caffeine consumption during early pregnancy impairs oviductal embryo transport, embryonic development and uterine receptivity in mice** *Biol Reprod* **99**:1266–1275

11. Klionsky D.J (2007) **Autophagy: from phenomenology to molecular understanding in less than a decade** *Nat Rev Mol Cell Biol* **8**:931–7

12. Wen X., Klionsky D.J. (2016) **An overview of macroautophagy in yeast** *J Mol Biol* **428**:1681–99

13. Itakura E., et al. (2008) **Beclin 1 forms two distinct phosphatidylinositol 3-kinase complexes with mammalian Atg14 and UVRAG** *Mol Biol Cell* **19**:5360–72

14. Sun Q., et al. (2008) **Identification of Barkor as a mammalian autophagy-specific factor for Beclin 1 and class III phosphatidylinositol 3-kinase** *Proc Natl Acad Sci U S A* **105**:19211–6

15. Wang Y.Y., Liu X.L., Zhao R. (2019) **Induction of Pyroptosis and Its Implications in Cancer Management** *Front Oncol* **9**

16. Man S.M., Karki R., Kanneganti T.D. (2017) **Molecular mechanisms and functions of pyroptosis, inflammatory caspases and inflammasomes in infectious diseases** *Immunol Rev* **277**:61–75

17. Wei X., et al. (2022) **Role of pyroptosis in inflammation and cancer** *Cell Mol Immunol* **19**:971–992

18. Lin L., et al. (2021) **Autophagy, Pyroptosis, and Ferroptosis: New Regulatory Mechanisms for Atherosclerosis** *Front Cell Dev Biol* **9**

19. Li X., et al. (2024) **Autophagy, Pyroptosis and Ferroptosis are Rising Stars in the Pathogenesis of Diabetic Nephropathy** *Diabetes Metab Syndr Obes* **17**:1289–1299

20. Zhao H., et al. (2022) **The Role of Autophagy and Pyroptosis in Liver Disorders** *Int J Mol Sci* **23**

21. Kong Y., et al. (2019) **The Natural Flavonoid Galangin Elicits Apoptosis, Pyroptosis, and Autophagy in Glioblastoma** *Front Oncol* **9**

22. Kim J.Y., et al. (2015) **Streptococcus pneumoniae induces pyroptosis through the regulation of autophagy in murine microglia** *Oncotarget* **6**:44161–78

23. Song Z.H., et al. (2015) **Germ cell-specific Atg7 knockout results in primary ovarian insufficiency in female mice** *Cell Death Dis* **6**

24. Gawriluk T.R., et al. (2014) **Beclin-1 deficiency in the murine ovary results in the reduction of progesterone production to promote preterm labor** *Proc Natl Acad Sci U S A* **111**:E4194–203

25. Oestreich A.K., et al. (2020) **The autophagy protein, FIP200 (RB1CC1) mediates progesterone responses governing uterine receptivity and decidualizationdagger** *Biol Reprod* **102**:843–851

26. Popli P., et al. (2023) **Beclin-1-dependent autophagy, but not apoptosis, is critical for stem-cell-mediated endometrial programming and the establishment of pregnancy** *Dev Cell* **58**:885–897

27. Oestreich A.K., et al. (2020) **The Autophagy Gene Atg16L1 is Necessary for Endometrial Decidualization** *Endocrinology* **161**

28. Matsunaga K., et al. (2009) **Two Beclin 1-binding proteins, Atg14L and Rubicon, reciprocally regulate autophagy at different stages** *Nat Cell Biol* **11**:385–96

29. Soyal S.M., et al. (2005) **Cre-mediated recombination in cell lineages that express the progesterone receptor** *Genesis* **41**:58–66

30. Zhang Y., et al. (2007) **A transgenic FOXJ1-Cre system for gene inactivation in ciliated epithelial cells** *Am J Respir Cell Mol Biol* **36**:515–9

31. Chadchan S.B., et al. (2019) **Antibiotic therapy with metronidazole reduces endometriosis disease progression in mice: a potential role for gut microbiota** *Hum Reprod* **34**:1106–1116

32. Chojnacki A.K., et al. (2023) **Tissue imaging reveals disruption of epithelial mitochondrial networks and loss of mitochondria-associated cytochrome-C in inflamed human and murine colon** *Mitochondrion* **68**:44–59

33. Kommagani R., et al. (2016) **The Promyelocytic Leukemia Zinc Finger Transcription Factor Is Critical for Human Endometrial Stromal Cell Decidualization** *PLoS Genet* **12**

34. Teng J.F., et al. (2020) **Polyphyllin VI Induces Caspase-1-Mediated Pyroptosis via the Induction of ROS/NF-kappaB/NLRP3/GSDMD Signal Axis in Non-Small Cell Lung Cancer** *Cancers (Basel* **12**

35. Tong W., Pollard J.W. (1999) **Progesterone inhibits estrogen-induced cyclin D1 and cdk4 nuclear translocation, cyclin E- and cyclin A-cdk2 kinase activation, and cell proliferation in uterine epithelial cells in mice** *Mol Cell Biol* **19**:2251–64

36. Ito S., Yamamoto Y., Kimura K. (2020) **Analysis of ciliogenesis process in the bovine oviduct based on immunohistochemical classification** *Mol Biol Rep* **47**:1003–1012

37. Liu Q., et al. (2018) **The role of mitochondria in NLRP3 inflammasome activation** *Mol Immunol* **103**:115–124

38. Shi Y., et al. (2022) **Echinacoside Induces Mitochondria-Mediated Pyroptosis through Raf/MEK/ERK Signaling in Non-Small Cell Lung Cancer Cells** *J Immunol Res, 2022*

39. Wang Y., et al. (2019) **Mitochondrial ROS promote macrophage pyroptosis by inducing GSDMD oxidation** *J Mol Cell Biol* **11**:1069–1082

40. Popli P., Sun A.J., Kommagani R. (2022) **The Multifaceted Role of Autophagy in Endometrium Homeostasis and Disease** *Reprod Sci* **29**:1054–1067

41. Choi J., et al. (2014) **Differential induction of autophagy by mTOR is associated with abnormal apoptosis in ovarian endometriotic cysts** *Mol Hum Reprod* **20**:309–17

42. Zhou S., et al. (2020) **Author Correction: Menopause-induced uterine epithelium atrophy results from arachidonic acid/prostaglandin E2 axis inhibition-mediated autophagic cell death** *Sci Rep* **10**

43. Fan W., Nassiri A., Zhong Q. (2011) **Autophagosome targeting and membrane curvature sensing by Barkor/Atg14(L)** *Proc Natl Acad Sci U S A* **108**:7769–74

44. Diao J., et al. (2015) **ATG14 promotes membrane tethering and fusion of autophagosomes to endolysosomes** *Nature* **520**:563–6

45. Ma X., et al. (2021) **LPS Mediates Bovine Endometrial Epithelial Cell Pyroptosis Directly Through Both NLRP3 Classical and Non-Classical Inflammasome Pathways** *Front Immunol* **12**

46. Cookson B.T., Brennan M.A. (2001) **Pro-inflammatory programmed cell death** *Trends Microbiol* **9**:113–4

47. Jorgensen I., Miao E.A. (2015) **Pyroptotic cell death defends against intracellular pathogens** *Immunol Rev* **265**:130–42

48. Liu J., et al. (2021) **Autophagy blockage promotes the pyroptosis of ox-LDL-treated macrophages by modulating the p62/Nrf2/ARE axis** *J Physiol Biochem* **77**:419–429

49. Lu Q., et al. (2016) **Homeostatic Control of Innate Lung Inflammation by Vici Syndrome Gene Epg5 and Additional Autophagy Genes Promotes Influenza Pathogenesis** *Cell Host Microbe* **19**:102–13

50. Netea-Maier R.T., et al. (2016) **Modulation of inflammation by autophagy: Consequences for human disease** *Autophagy* **12**:245–60

51. Finnerty R.M., et al. (2024) **Multi-omics analyses and machine learning prediction of oviductal responses in the presence of gametes and embryos** *bioRxiv*

Author information

Pooja Popli
Department of Pathology and Immunology, Baylor College of Medicine, Houston, USA

Arin K Oestreich
Department Obstetrics and Gynecology, Washington University School of Medicine, St. Louis, USA, Center for Reproductive Health Sciences, Washington University School of Medicine, St. Louis, USA

Vineet K Maurya
Department of Molecular and Cellular Biology, Baylor College of Medicine, Houston, USA

Marina N Rowen
Department Obstetrics and Gynecology, Washington University School of Medicine, St. Louis, USA, Center for Reproductive Health Sciences, Washington University School of Medicine, St. Louis, USA

Yong Zhang
Department of Medicine and Department of Cell Biology, Washington University School of Medicine, St. Louis, USA

Michael J Holtzman
Department of Medicine and Department of Cell Biology, Washington University School of Medicine, St. Louis, USA

Ramya Masand
Department of Pathology and Immunology, Baylor College of Medicine, Houston, USA

John Lydon
Department of Molecular and Cellular Biology, Baylor College of Medicine, Houston, USA

Shizuo Akira
Department of Host Defense, Research Institute for Microbial Diseases (RIMD), Osaka University, Osaka, Japan, Laboratory of Host Defense, World Premier Institute Immunology Frontier Research Center (WPI-IFReC), Osaka University, Osaka, Japan

Kelle H Moley
Department Obstetrics and Gynecology, Washington University School of Medicine, St. Louis, USA, Center for Reproductive Health Sciences, Washington University School of Medicine, St. Louis, USA

Ramakrishna Kommagani
Department of Pathology and Immunology, Baylor College of Medicine, Houston, USA, Department of Molecular Virology and Microbiology, Baylor College of Medicine, Houston, USA
ORCID iD: 0000-0003-0403-0971

For correspondence: Rama.Kommagani@bcm.edu

Editors

Reviewing Editor
Wei Yan
Washington State University, Pullman, United States of America

Senior Editor
Wei Yan
Washington State University, Pullman, United States of America

Reviewer #1 (Public review):

This study by Popli et al. evaluated the function of Atg14, an autophagy protein, in reproductive function using a conditional knockout mouse model. The authors showed that female mice lacking Atg14 were infertile partly due to defective embryo transport function of the oviduct and faulty uterine receptivity and decidualization using PgrCre/+;Atg14f/f mice. The findings from this work are exciting and novel. The authors demonstrated that a loss of Atg14 led to an excessive pyroptosis in the oviductal epithelial cells that compromises cellular integrity and structure, impeding the transport function of the oviduct. In addition, the authors use both genetic and pharmacological approaches to test the hypothesis. Therefore, the findings from this study are high-impact and likely reproducible. However, there are multiple major concerns that need to be addressed to improve the quality of the work.

https://doi.org/10.7554/eLife.97325.2.sa3

Reviewer #2 (Public review):

In this manuscript, Popli et al investigated the roles of autophagy related gene, Atg14, in the female reproductive tract (FRT) using conditional knockout mouse models. By ablation of Atg14 in both oviduct and uterus with PR-Cre (Atg14 cKO), authors discovered that such females are completely infertile. They went on to show that Atg14 cKO females have impaired embryo implantation as well as embryo transport from oviduct to uterus. Further analysis showed that Atg14 cKO leads to increased pyroptosis in oviduct, which disrupts oviduct epithelial integrity and leads to obstructive oviduct lumen and impaired embryo transport. The authors concluded that Atg14 is critical for maintaining the oviduct homeostasis and keeping the inflammation under check to enable proper embryo transport.

The authors have barely addressed most of my concerns in this revised version with a few minor issues remaining to be addressed:

(1) The authors tried to address my first concern regarding the statement that "autophagy is critical for maintaining the oviduct homeostasis". The revised statement in Line 53-54 "we report that Atg14-dependent autophagy plays a crucial role in maintaining..." is still not correct. It should be corrected as " we report that autophagy-related protein Atg14 plays a crucial role in maintaining...".
(2) Line 349-351 described 80-90% of blastocysts retrieved from oviducts of cKO mice, which is in consistent with Figure 3B (showing more than 98%).
(3) Line 447, "Fig. 5E" should be Fig. 6A. In addition, grammar error in the next sentence.
(4) In Figure 6D, why the composition of blastocysts in chemical treated group do not add up to 100%.

https://doi.org/10.7554/eLife.97325.2.sa2

Reviewer #3 (Public review):

Summary:

The manuscript by Pooja Popli and co-authors tested the importance of Atg14 in the female reproductive tract by conditionally deleting Atg14 use PrCre and also Foxj1cre. The authors showed that loss of Atg14 leads to infertility due to the retention of embryos within the oviduct. The authors further concluded that the retention of embryos within the oviduct is due to pyroptosis in oviduct cells leading to defective cellular integrity. The revised manuscript has included new experimental data (Figs. S2B, 5B, 5C, and S3) that satisfied the concerns of this reviewer. The manuscript should provide important advancement to the field.

https://doi.org/10.7554/eLife.97325.2.sa1

Author response:

The following is the authors' response to the original reviews.

We greatly appreciate the opportunity to submit a revision of our manuscript entitled: "The Autophagy Protein, ATG14 Safeguards Against Unscheduled Pyroptosis Activation to Enable Embryo Transport During Early Pregnancy" by Popli et al. We thank all three Referees for underscoring the importance of our findings as well as the constructive critiques that we used to improve our paper. Most notably, we added the following new data:

· To provide more insight into whether pyroptosis activation occurs distinctly in the oviduct, we looked for GSDMD, (primary executioner of the pyroptosis pathway) expression in the uterus and ovary too. We observed no signs of pyroptosis activation in response to ATG14 loss in either the uterus or ovary of *Atg14* cKO mice compared to control ones suggesting that ATG14 plays a distinct role in regulating pyroptosis specifically in the oviduct (Revised Figure 5F).

· To better understand the molecular mechanisms of pyroptosis activation in the oviducts, we examined various key markers of mitochondrial integrity, architecture, and function in control and *Atg14* cKO oviducts. Our findings indicate a significant loss of mitochondrial structural and functional integrity, possibly contributing to the embryo retention phenotype via activating the pyroptosis pathway in the oviduct. (Revised Figure 5B & C).

· To address the spatiotemporal and region-specific expression of ATG14 in the oviduct, we performed immunofluorescence analysis and observed the consistent expression of ATG14 in all the cellular compartments of oviducts including ciliary epithelial cells, secretory epithelial cells, and smooth muscle cells. Moreover, the region-specific expression analysis revealed

that distinct expression of ATG14 in the ampullary region of cKO mice oviduct helps to preserve its structural integrity. Conversely, its loss in the isthmus region of the oviduct in concordance with active PR-cre activity causes completely distorted epithelial structures with luminal obliteration or narrowing resulting in an unorganized and obstructed lumen leading to embryo retention, suggesting that ATG14 is essential for maintaining the structural integrity of the oviduct (Revised Figure 3F & S2A).

· Considering the expression of PR-cre in the pituitary, which could potentially influence hormonal secretion and ovulation, we evaluated the levels of E2 and P4 during pregnancy. Our findings show that these hormone levels remained unchanged in *Atg14* cKO mice, indicating that the absence of ATG14 does not negatively affect the HPG axis or pituitary function (Revised Figure 2F).

· ATG14 is an essential factor for the initiation of autophagy, and its loss can lead to reduced or inhibited autophagic activity. Consistently, we observed elevated levels of LC3b and p62 proteins, two well-known markers of autophagic flux in the oviducts of *Atg14*-deficient mice implying that loss of ATG14 leads to defective autophagy potentially disturbing the structural integrity of oviductal epithelial cells and impairing embryo transport. (New Supplementary Figure S2B).

> ***Reviewer #1 (Public Review):***
>
> *This study by Popli et al. evaluated the function of Atg14, an autophagy protein, in reproductive function using a conditional knockout mouse model. The authors showed that female mice lacking Atg14 were infertile partly due to defective embryo transport function of the oviduct and faulty uterine receptivity and decidualization using PgrCre/+; Atg14f/f mice. The findings from this work are exciting and novel. The authors demonstrated that a loss of Atg14 led to an excessive pyroptosis in the oviductal epithelial cells that compromises cellular integrity and structure, impeding the transport function of the oviduct. In addition, the authors use both genetic and pharmacological approaches to test the hypothesis. Therefore, the findings from this study are high-impact and likely reproducible. However, there are multiple major concerns that need to be addressed to improve the quality of the work.*
>
> *Major comments:*
>
> *(1) It is interesting that deletion of Atg14 using PgrCre results in pyroptosis only in the oviduct; the authors should speculate/evaluate why the oviduct, but not the uterus or follicles. Is there any cellular specificity that is sensitive to autophagy/pyroptosis in the oviduct but not in other cell types? This has not been evaluated or discussed in the manuscript. Is it possible to include GSDMD IHC for the uterine section to ensure that there was no pyroptosis event in the cKO uteri?*

We performed GSDMD IHC and found that, unlike in the oviduct, the cKO uteri and ovaries do not exhibit detectable pyroptosis (Revised Figure 5F). Additionally, we have added text to the discussion section addressing possible reasons for the differential impact of Atg14 loss on pyroptosis along the reproductive tract continuum (Line number: 532-538)

> *(2) Please include an explanation of how a loss of Atg14, important for the initiation process of autophagy (as indicated in line 88), can lead to pyroptosis. There was some discussion about inflammation. But the connection is still missing.*

We thank the reviewer for noting on this. We have now included a possible explanation of how autophagy could impact pyroptosis in the discussion section (Line number: 532-538)

> *(3) No expression data of ATG14 using IHC/IF analysis were included in the manuscript - this is missing. This is needed and important as the authors found that Foxj1Cre/+; Atg14f/f cKO mice had no fertility defect. Is it possible that ATG14 is not present in the ciliated epithelial cells of the oviduct? In addition, the data in Figure 5B also points to this speculation. This is because the GSDMD (the pyroptosis marker) is only observed in the isthmus region but not the ampulla.*

We thank the reviewer for this nice suggestion. We performed the immunofluorescence analysis for ATG14 expression in control and *Atg14* cKO oviducts and observed the consistent expression of ATG14 in all the cellular compartments of oviducts including ciliary epithelial cells, secretory epithelial cells, and smooth muscle cells (New Supplementary Figure S2A). We also looked for α-tubulin expressions in the oviduct of Foxj1Cre/+; Atg14 f/f mice and control mice and observed that ciliated epithelial cells that were positive for acetylated α-tubulin staining did not appear to be different in Foxj1Cre/+; Atg14 f/f mice oviduct compared to controls (Revised Figure 4C). However, due to the unavailability of reliable fluorescent-labeled antibodies for both Foxj1 and Atg14, we were unable to conduct the co-localization study as intended. This limitation hindered our ability to precisely determine the spatial overlap of these proteins within the tissue.

> *(4) In line with the previous comment, is ATG14 present in the human Fallopian tube? If so, which cell type? This needs to be addressed.*

Author's Response: We appreciate the reviewer's valuable suggestion. While we currently lack access to human fallopian tube biopsies, the Human Protein Atlas (https://www.proteinatlas.org/ENSG00000126775-ATG14) demonstrates distinct ATG14 expression in various fallopian tube cell types, with localization in the cytoplasm, membrane, and nucleus.

> *(5) As PgrCre is also expressed in the pituitary, is it possible that the deletion of Atg14 using PgrCre would affect pituitary function – hence a change in the FSH/LH secretion that subsequently affects ovulation? Although the uterine and ovarian histology in the Atg14 cKO looks similar to the controls, is it possible that cyclicity is also affected? The authors should evaluate whether the estrous cycle takes place regularly.*

Author's Response: Thank you for the insightful comment. However, evaluating the estrous cycle requires significant time and effort and is beyond the scope of the current manuscript. Nonetheless, we have now shown that both P4 and E2 levels were not altered in *Atg14* cKO mice, indicating that the loss of Atg14 did not adversely impact the HPG axis, and by extension, pituitary function (Revised Figure 2F).

> *(6) The number of total embryos/oocytes in the cKO compared to the control has not been evaluated - this data must be included. Do the changes in autophagy in Atg14 cKO affect preimplantation embryo development? Please categorize the embryos found in the oviduct/uterus in both genotypes. i.e., % blastocyst, % morula, % developmentally delayed, % non-viable etc. It would be interesting to evaluate if the oviduct with heavy pyroptosis can support preimplantation embryo development.*

Author's Response: We thank the reviewer for this nice suggestion. We categorized the embryos into different categories as suggested and included the data (Revised Figure 3C and Figure 6D).

> *(7) It is unclear why the superovulation+mating experiment (Figure 3C) was performed. Please provide justification. Why was the data from natural mating (Figure 3A) insufficient?*

Author's Response: In Figure 3C, superovulation was employed to complement the natural mating studies and to provide stronger evidence for the embryo retention phenotype observed in the oviduct.

> *(8) In lines 297-298, the conclusion that "ATG14 is required for P4-mediated but not for E2-mediated actions during uterine receptivity" is not entirely correct. This is because the authors also observed that the downregulation of MUC1 (E2-target protein) is absent in the PgrCre/+;Atg14f/f cKO female uteri.*

We thank the reviewer for noting this. We detected more E2-induced targets in D-4 pregnant uterine samples and found no change in their expression in response to *Atg14* depletion in cKO females (Revised Figure 2E).

> *(9) Figure 3D: Please include an image that also represents the ampulla region. All images are from the isthmus region. It would be informative to see if the loss of cell boundaries also takes place at the ampulla region in the cKO oviduct.*

We thank the reviewer for this nice suggestion. We included the ampulla section from the cKO and control female oviducts (Revised Figure 3F). As PR-cre activity is limited to isthmus only [1, 2], we did not see any structural abnormality in ampulla sections of cKO oviducts.

> *(10) Figure 3E: Please indicate which region the TEM was performed. Isthmus? Ampulla? Were the changes in mitochondrial phenotype observed across all oviductal regions?*

The TEM imaging was performed by the WashU Core services. Although we clearly mentioned the core person to look into the isthmus region only, we are not sure if they accurately follow the instructions.

> *(11) Figure 4B; the evaluation of FOXJ1 IHC. The authors need to include sections that also have an ampulla region-especially in the cKO. In addition, it is misleading to state that there were fewer FOXJ1+ cells (line 361) in the cKO if the region being evaluated is the isthmus (which has a lot fewer ciliated epithelial cells in general) while the control image showed an ampulla where the abundancy of ciliated epithelial cells (FOXJ1+) is higher than that of the isthmus. The authors also need to include a higher resolution image (a zoom-in at the ciliated epithelial cells with FOXJ1+ signal) as well as the quantification of FOXJ1+ cells.*

We appreciate the reviewer for the suggestion. In Figure 4A, we have already shown the ampulla region from both control and cKO oviducts, wherein alpha-tubulin staining was evident in both oviducts.

We agree with the reviewer that the isthmus usually has fewer ciliary epithelial cells than the ampulla, however, as illustrated in Figures 4A and 4B, *Atg14* depletion causes a marked disruption of structural integrity with loss of cell boundaries specifically in the isthmus, which is far more pronounced than in the ampulla. One reason for this is the reported Pgr Cre activity, which is much more robust in the isthmus than in the ampulla [1, 2] . This disruption leads to the substantial loss of both ciliated and secretory cells, compromising the epithelial architecture to such an extent that it is impossible to accurately quantify the Foxj1 signal as can be seen in higher resolution images in New Supplementary Figure S3.

For more clarity, we modified the statement in the revised file (Line Number: 393-396)

> *(12) All IHC/IF and embryo images need to include the scale bars.*

We thank the reviewer for this suggestion. We now included the scale bar in all the images.

> *(13) Figure 5H: although IL1B is being discussed, there was no data in this study to support the figure.*

In Figure 5H, IL1B is presented as part of the pyroptosis signaling pathway. As we have already shown other key executioners of this pathway: Caspase 1 and GSDMD, we believe that additional IL1B data would not provide new insights beyond what has already been shown.

> *Minor comments:*
>
> *(1) Please include n (sample size) for all data, including the histology image in the figure legends for all studies.*

We now included the sample size in figure legends for all data shown in the manuscript.

> *(2) Line 32, did the authors mean to say, "Self-digestion of..." instead of "Self-digestion for..."?*

In Line 32, we meant, “Cellular self-digestion for female reproductive tract functions”. We have now corrected the statement.

> *Fig. 1A - please include negative control.*

We included the negative control (Revised Figure 1)

> *(3) Figure 1E left panel and Figure 4C - please label "Average no. of pups/female/litter" as each female has more than one litter over her reproductive lifespan. If the authors represent pups/females, then the number should be accumulative in the range of 35-40pups/females in the control group.*

We thank the reviewer for noting this. We now corrected the label in both Revised Figure 1E and Revised Figure 4E.

> *(4) Line 273: please remove "& F" as there is no Figure F in the image.*

We removed “&F” from the Line 273.

> *(5) The presence of CL is not always indicative of normal hormonal levels; therefore, the authors should include the measurement of progesterone levels at 3.5 dpc in the cKO compared to the control group. Hormonal regulation is also crucial for embryo transport.*

We thank the reviewer for this suggestion. We measured not only P4 but also E2 levels in D4 pregnant females and found no significant difference in their levels compared to corresponding controls (Revised Figure 2F).

> *(6) Figure 2A shows that KRT expression is not present in the control uteri. Although the KRT8 levels may have decreased at 4 dpc, they should be present (see Figure S2A).*

We observed no decrease in KRT expression in control uteri on 5 dpc. We included better-resolution images for KRT expression (Revised Figure 2A).

> *(7) The dotted white lines in Figure 2A are too thick. It's difficult to see the Ki67 positive signal in the luminal epithelial cells. Please also add a quantitative analysis of Ki67+ cells in the luminal epithelium vs. stromal cells.*

We now corrected the dotted lines in Revised Figure 2B. However, as the Ki-67 proliferation is evident in the representative images, we believe quantification analysis will not add anything new to the existing conclusion.

> *(8) Figure 2D - the y-axis mentions the weight ratio. However, the figure legend describes the transcript levels of Atg14 - please correct this.*

We corrected the label in the revised manuscript.

> *(9) Line 294 - Please correct Figure 2C to Figure 2B.*

We corrected it.

> *(10) Line 308 - Please correct Figure 2E to Figure 2F.*

We corrected it.

> *(11) Line 310 - Please correct Figure 2F to Figure 2G.*

We corrected it.

> *(12) Line 311 - Please correct Figure 2F to Figure 2G.*

We corrected it.

> *(13) Information in Figure S2A and S2B should be included in the main figure.*

We thank the reviewer for this nice suggestion. We now included the figures S2A and S2B in the main figure (Revised Figure 2C & D).

> *(14) Figure 3C - due to a lot of cellular debris after flushing, it's difficult to see. But it seems like there are secondary follicles in the flushing of control oviducts - this is highly unlikely. This could be due to an artifact of an accidental poking of the ovaries during collection.*

We agree with the reviewer. It might be due to the unintentional poking of the ovaries. We will take extra care in future experiments to avoid this and ensure clean flushing to prevent any confusion from debris or artifacts.

> *(15) Figure 2B and Figure 3D signals from DAPI are missing - it's black with no blue signal. This could be the data loss during file compression for manuscript submission.*

We included better-resolution pictures for the DAPI signal in Revised Figure 2B & Figure 3F.

> *(16) Explain why some embryos in the cKO make it to the uterus when the females are superovulated.*

It might be due to the heightened hormonal stimulation provided by the superovulation which could facilitate the movement of some embryos through the oviduct despite any

defects or abnormalities caused by the loss of ATG14 in the oviduct.

> ***Reviewer #2 (Public Review):***
>
> *Summary:*
>
> *In this manuscript, Popli et al investigated the roles of the autophagy-related gene, Atg14, in the female reproductive tract (FRT) using conditional knockout mouse models. By ablation of Atg14 in both oviduct and uterus with PR-Cre (Atg14 cKO), the authors discovered that such females are completely infertile. They went on to show that Atg14 cKO females have impaired embryo implantation and uterus receptivity due to impaired response to P4 stimulation and stromal decidualization. In addition to the uterus defect, the authors also discovered that early embryos are trapped inside the oviduct and cannot be efficiently transported to the uterus in these females. They went on to show that oviduct epithelium in Atg14 cKO females showed increased pyroptosis, which disrupts oviduct epithelial integrity and leads to obstructive oviduct lumen and impaired embryo transport. Therefore, the authors concluded that autophagy is critical for maintaining the oviduct homeostasis and keeping the inflammation under check to enable proper embryo transport.*
>
> *Strengths:*
>
> *This study revealed an important and unexpected role of the autophagy-related gene Atg14 in preventing pyroptosis and maintaining oviduct epithelial integrity, which is poorly studied in the field of reproductive biology. The study is well designed to test the roles ofATG14 in mouse oviduct and uterus. The experimental data in general support the conclusion and the interpretations are mostly accurate. This work should be of interest to reproductive biologists and scientists in the field of autophagy and pyroptosis.*
>
> *Weaknesses:*
>
> *Despite the strengths, there are several major weaknesses raising concerns. In addition, the mismatched figure panels, the undefined acronyms, and the poor description/presentation of some of the data significantly hinder the readability of the manuscript.*
>
> *(1) In the abstract, the authors stated that "autophagy is critical for maintaining the oviduct homeostasis and keeping the inflammation under check to enable embryo transport". This statement is not substantiated. Although Atg14 is an autophagy-related gene and plays a critical role in oviduct homeostasis, the authors did not show a direct link between autophagy and pyroptosis/oviduct integrity. In addition, the authors pointed out in the last paragraph of the introduction that none of the other autophagy-related genes (ATG16L, FIP200, BECN1) exhibited any discernable impact on oviduct function. Therefore, the oviduct defect is caused by Atg14 specifically, not necessarily by autophagy.*

We thank the reviewer for noting this. We corrected the statement in the revised manuscript (Line number: 53-54).

> *(2) In lines 412-414, the authors stated that "Atg14 ablation in the oviduct causes activation of pyroptosis", which is also not supported by the experimental data. The authors did not show that Atg14 is expressed in oviduct cells. PR-Cre is also not specific in oviduct cells. It is possible that Atg14 knockout in other PR-expressing tissues (such as the uterus) indirectly activates pyroptosis in the oviduct. More experiments will be required to support this claim. In line with the no defect when Atg14 has knocked out in oviduct ciliary cells, it will be good to use the secretory cells Cre, such as Pax8-Cre, to*

> *demonstrate that Atg14 functions in the secretory cells of the oviduct thus supporting this conclusion.*

We now included the ATG14 expression data in the oviduct (New Supplementary Figure S2A). Consistent with previous studies reporting PR-cre activity in the isthmus [1, 2] , we observed that *Atg14* depletion was more pronounced in the isthmus compared to the ampulla. However, generating a secretory Pax-8 cell Cre mice model will require a substantial amount of time and effort, and we respectfully note that this is beyond the scope of the current manuscript.

> *(3) With FOXJ1-Cre, the authors attempted to specifically knockout Atg14 in ciliary cells, but there are no clear fertility and embryo implantation defects in Foxj1/Atg14 cKO mice. The author should provide verification data to show that Atg14 had been effectively depleted in ciliary cells if Atg14 is normally expressed.*

We understand the reviewer's concern. We included new data for ATG14 expression in control and *Atg14* cKO mice oviducts (New Supplementary Figure S2A). However, due to the unavailability of reliable fluorescent-labeled antibodies for both Foxj1 and Atg14, we could not conduct the co-localization studies as intended, and this limitation hindered our ability to precisely determine the spatial overlap of these proteins within the oviduct. Nonetheless, Foxj1-cre is a widely used mice model with reported cre-activity in ciliary epithelial cells including oviduct tissues [3]. Given the widespread expression of ATG14 in all the ciliary and secretory cells (New Supplementary Figure S2A) and distinct FOXJ1 expression in the oviduct (New Supplementary Figure S3), we are confident that Atg14 is deleted in the ciliary epithelial cells of *Foxj1*|*Atg14* cKO mice oviducts.

> *(4) In lines 307-313, the author tested whether ATG14 is required for the decidualization of HESCs. The author stated that "Control siRNA transfected cells when treated with EPC seemed to change their morphological transformation from fibroblastic to epithelioid (Fig. 2E) and had increased expression of the decidualization markers IGFBP1 and PRL by day three only (Fig. 2F)". First, the labels in Figure 2 are not corresponding to the description in the text. Second, the morphology of the HESCs in the control and Atg14 siRNA group showed no obvious difference even at day 3 and day 6. The author should point out the difference in each panel and explain in the text or figure legend.*

Decidualization is a post-implantation event, whereas our study primarily focuses on pre-implantation events in the oviduct. Therefore, we have removed all data related to human and mouse decidualization to enhance the clarity and precision of our study.

> *(5) In lines 332-336, the authors pointed out that the cKO mice oviduct lining shows marked eosinophilic cytoplasmic change, but there's no data to support the claim. In addition, the authors further described that "some of the cells showed degenerative changes with cytoplasmic vacuolization and nuclear pyknosis, loss of nuclear polarity, and loss of distinct cell borders giving an appearance of fusion of cells (Fig. 3D)". First, Figure 3D did not show all these phenotypes, and it is likely a mismatch to Figure 3E. Even in Figure 3E, it is not obvious to notice all the phenotypes described here. The figure legend is overly simple, and there's no explanation of the arrowheads in the panel. More data/images are required to support the claim here and provide a clear indication and explanation in the figure legend.*

Dr. Ramya Masand, Chief pathologist in the Pathology Department at the Baylor College of Medicine, and a contributing author, assessed the H&E-stained oviduct sections from control and cKO mice. We have now included a new Supplementary Figure S3 with previous representative H&E images that depict the cellular alterations described in lines 332–336.

> *(6) In lines 317-325, it is rather confusing about the description of the portion of embryos from the oviduct and uterus. In addition, the total number of embryos was not provided. I would recommend presenting the numerical data to show the average embryos from the oviduct and uterus instead of using the percentage data in Figures 3A and 5G.*

We thank the reviewer for this nice suggestion. We calculated the average number of embryos and found no difference in the number of embryos recovered from cKO or polyphyllin-treated pregnant mice at 4 dpc compared to their controls. (New Supplementary Figure S4A & B).

> *(7) In lines 389-391, authors tested whether Polyphyllin VI treatment led to activated pyroptosis and blocked embryo transport. Although Figures 5F-G showed the expected embryo transport defect, the authors did not show the pyroptosis and oviduct morphology. It will be important to show that the Polyphyllin VI treatment indeed led to oviduct pyroptosis and lumen disruption.*

We performed the GSDMD staining IHC in Polyphyllin VI or vehicle-treated mice oviducts and observed elevated GSDMD expression with Polyphyllin V (New Figure 6E). However, no significant lumen disruption was detected, which may be attributed to the short-term exposure of the oviducts to pyroptosis induction, in contrast to the more pleiotropic effects observed in genetically induced models. Nonetheless, this observation clearly indicates that unscheduled or unwarranted activation of pyroptosis impedes embryo transport.

> *(8) In line 378, it would be better to include a description of pyroptosis and its molecular mechanisms to help readers better understand your experiments. Alternatively, you can add it in the introduction.*

We thank the reviewer for this nice suggestion. We included literature on the pyroptosis pathway in the introduction section (Line Number: 105-118).

> *(9) Please make sure to provide definitions for the acronyms such as FRT, HESCs, GSDMD, etc.*

We added definitions for the acronyms such as FRT, HESCs, and GSDMD used in the study.

> *(10) It is rather confusing to use oviducal cell plasticity in this manuscript. The work illustrated the oviducal epithelial integrity, not the plasticity.*

We thank the reviewer for the suggestion. We have revised the manuscript accordingly to ensure clarity and precision in describing the oviductal epithelial structural changes observed in the absence of ATG14.

> *A few of the additional comments for authors to consider improving the manuscript are listed below.*
>
> *(1) Some of the figures are missing scale bars, while others have inconsistent scale bars. It would be better to be consistent.*

We now included the scale bars in all images.

> *(2) On a couple of occasions, the DAPI signal cannot be seen, such as in Figure 2B and Figure 3D.*

We now included better-resolution images for the DAPI signal in all fluorescent images shown in the revised manuscript.

> *(3) Overall, the figure legends can be improved to provide more detailed information to help the reader to interpret the data.*

We included additional details in all the figure legends in the revised manuscript.

> *(4) In Figure 2D, the Y-axis showed the stimulated/unstimulated uterine weight ratio, why did the author put "Atg14" at the top of the graph? At the same time, the X-axis title is missing in Figure 2D.*

We apologize for the typo error. We removed “Atg14” from the top of the graph and included the X-axis title in the revised manuscript.

> *(5) In the left panel of Figure 2G, "ATG14" at the top should be "Atg14" to be consistent.*

In Figure 2G, we are representing “ATG14” according to human gene annotation.

> *(6) In line 559, there miss "(A)" in front of Immunofluorescence analysis of GSDMD.*

We thank the reviewer for noting this. We corrected it in the revised manuscript.

> ***Reviewer #3 (Public Review):***
>
> *Summary:*
>
> *The manuscript by Pooja Popli and co-authors tested the importance of Atg14 in the female reproductive tract by conditionally deleting Atg14 using Pr Cre and also Foxj1cre. The authors showed that loss of Atg14 leads to infertility due to the retention of embryos within the oviduct. The authors further concluded that the retention of embryos within the oviduct is due to pyroptosis in oviduct cells leading to defective cellular integrity. The manuscript has some interesting findings, however there are also areas that could be improved.*
>
> *Strengths:*
>
> *The importance of Atg14 and autophagy in the female reproductive tract is incompletely understood. The manuscript also provide spatial evidence about a new mechanism linking Atg14 to pyroptosis.*

We thank the reviewer for the positive statements and constructive comments on our manuscript.

> *Weaknesses:*
>
> *(1) It is not clear why the loss of Atg14 selectively induces Pyroptosis within oviduct cells but not in other cellular compartments. The authors should demonstrate that these events are not happening in uterine cells.*

We thank the reviewer for this nice suggestion. We performed GSDMD IHC and found that, unlike in the oviduct, the cKO uteri and ovaries do not exhibit detectable pyroptosis (Revised Figure 5F). Additionally, we have added text to the discussion section addressing possible reasons for the differential impact of Atg14 loss on pyroptosis along the reproductive tract continuum (Line number: 532-538)

> *(2) The manuscript never showed any effect on the autophagy upon loss of Atg14. Is there any effect on autophagy upon Atg14 loss? If so, does that contribute to the observation?*

We thank the reviewer for the nice suggestion. We found LC3b and p62 protein levels, two well-known markers of autophagic flux are elevated due to Atg14 loss in the oviduct (New Supplementary Figure S2B). Since, p62 accumulation is an indicative of the reduced autophagic flux [4], we posit loss of Atg14 results in defective autophagy in the oviduct. Importantly, this defective autophagy adversely impacted the structural integrity of oviductal epithelial cells, causing impairment in embryo transport.

> *(3) It is not clear what the authors meant by cellular plasticity and integrity. There is no evidence provided in that aspect that the plasticity of oviduct cells is lost. Similarly, more experimental evidence is necessary for the conclusion about cellular integrity.*

We thank the reviewer for the suggestion. We have revised the text for clarity and precision in describing the oviductal epithelial structural changes observed in the absence of ATG14. To avoid ambiguity, we have removed the term "cellular plasticity." We have already provided extensive evidence, including multiple H&E stains and immunofluorescence analyses for KRT8 and smooth muscle actin to illustrate cellular integrity in both control and cKO oviducts. However, we respectfully believe that performing additional experiments on cellular integrity would not contribute further to the conclusions already drawn.

> *(4) The mitochondrial phenotype shown in Figure 3 didn't appear as severe as it is described in the results section. The analyses should be more thorough. They should include multiple frames (in supplemental information) showing mitochondrial morphology in multiple cells. The authors should also test that aspect in uterine cells. The authors should measure Feret's diagram. Diff erence in membrane potential etc. for a definitive conclusion.*

We appreciate the reviewer's suggestion. We carried out the TOM20 (mitochondrial structural marker) and cytochrome C (mitochondrial damage and cell death marker) immune-colocalization study and found loss of TOM20 signal with concomitant cytochrome c leakage into the peri-nuclear space (Revised Figure 5B). Additionally, we also observed reduced expression of mitochondrial structural and functional markers by qPCR analysis (Revised Figure 5C). However, we respectfully argue that conducting membrane potential studies on murine oviducts is extremely complex and is beyond the scope of this study.

> *(5) The comment that the loss of Atg14 and pyroptosis leads to the narrowing of the lumen in the oviduct should be experimentally shown.*

We have now included a New Supplementary Figure S3 with representative previous immunofluorescence images that clearly show the narrowing of the lumen with Atg14 loss in the oviduct.

> *(6) The manuscript never showed the proper mechanism through which Atg14 loss induces pyroptosis. The authors should link the mechanism.*

We respectfully disagree with the reviewer on this point. We have provided substantial evidence regarding the cellular mechanisms through which the loss of Atg14 may lead to the activation of pyroptosis as outlined below:

(1) Cellular Changes: Loss of ATG14 in the oviduct results in cellular swelling and the formation of fused membranous structures, which are characteristic features of pyroptosis activation.

(2) Expression of Key Pyroptosis Proteins: We observed an induced expression of GSDMD and Caspase-1, primary executioners of the pyroptotic pathway, in response to Atg14 loss.

(3) Inflammatory Markers: Elevated levels of inflammatory markers such as TNF-α and CXCR3 were detected, both of which are known to promote pyroptosis [5, 6].

(4) Mitochondrial Damage: We have added new data demonstrating disrupted colocalization of TOM20 (a mitochondrial structural marker) and Cytochrome c (a cell death marker), resulting in Cytochrome c leakage into the perinuclear space (Revised Figure 5B). Additionally, qPCR analysis revealed reduced expression of mitochondrial structural and functional markers in cKO oviduct tissues (Revised Figure 5C).

Based on these evidences, we can clearly say that Atg14 has some direct or indirect link to inflammasome activation. However, understanding the complex rheostat between the Atg14-mediated autophagy and inflammation regulatory axis will necessitate future studies employing sophisticated models, such as combined knockout mice where ATG14 is deleted alongside key inflammatory regulators (e.g., NLRP3, GSDMD, or CASPASE-1). These dual knockout models could provide crucial insights into how ATG14 modulates inflammatory pathways.

References:

(1) Herrera, G.G.B., et al., *Oviductal Retention of Embryos in Female Mice Lacking Estrogen Receptor alpha in the Isthmus and the Uterus.* Endocrinology, 2020. 161(2).

(2) Soyal, S.M., et al., *Cre-mediated recombination in cell lineages that express the progesterone receptor.* Genesis, 2005. 41(2): p. 58-66.

(3) Zhang, Y., et al., *A transgenic FOXJ1-Cre system for gene inactivation in ciliated epithelial cells.* Am J Respir Cell Mol Biol, 2007. 36(5): p. 515-9.

(4) Mizushima, N., T. Yoshimori, and B. Levine, *Methods in mammalian autophagy research.* Cell, 2010. 140(3): p. 313-26.

(5) Vaher, H., *Expanding the knowledge of tumour necrosis factor-alpha-induced gasdermin E-mediated pyroptosis in psoriasis.* Br J Dermatol, 2024. 191(3): p. 319-320.

(6) Liu, C., et al., *CXCR4-BTK axis mediate pyroptosis and lipid peroxidation in early brain injury after subarachnoid hemorrhage via NLRP3 inflammasome and NF-kappaB pathway.* Redox Biol, 2023. 68: p. 102960.

https://doi.org/10.7554/eLife.97325.2.sa0